JOURNAL OF GEOPHYSICAL RESEARCH, VOL. 114, F00A05, doi:10.1029/2009JF001267, 2009

Click Here for Full Article

Statistical description of slope-dependent soil transport and the diffusion-like coefficient

David Jon Furbish,[1] Peter K. Haff,[2] William E. Dietrich,[3] and Arjun M. Heimsath[4]

Received 15 January 2009; revised 12 April 2009; accepted 11 June 2009; published 22 September 2009.

[1] For hillslopes undergoing "diffusive" soil transport, it is often assumed that the soil flux is proportional to the local land-surface gradient, where the coefficient of proportionality is like a diffusion coefficient. Inasmuch as transport involves quasi-random soil particle motions related to biomechanical mixing and similar dilational processes, a slope-dependent relation arises from a balance between particle fluxes that tend to loft a soil and gravitational settling of particles into available pore space. A specialized form of the Fokker-Planck equation adapted to such particle motions clarifies how the particle flux involves advective and diffusive parts. This in turn contributes to a kinematic description of the diffusion-like coefficient. Ingredients of this coefficient include an active soil thickness, a characteristic particle size, the porosity in excess of a consolidated porosity, and the rate of particle activation as a function of depth. These last two ingredients, vertical porosity structure and activation rate, in effect characterize the magnitude and frequency of settling particle motions related to biological activity and thereby set the rate constant of the transport process. The significance of land-surface slope is that it is a measure of the downslope component of slope-normal lofting that is balanced by settling. Because the diffusion-like coefficient contains the soil thickness, the analysis suggests that the soil flux is proportional to the "depth-slope" product. The analysis is consistent with published profiles of soil creep displacement and with published estimates of soil flux obtained by downslope integration of soil production rates for hillslopes in California and Australia.

Citation: Furbish, D. J., P. K. Haff, W. E. Dietrich, and A. M. Heimsath (2009), Statistical description of slope-dependent soil transport and the diffusion-like coefficient, *J. Geophys. Res.*, *114*, F00A05, doi:10.1029/2009JF001267.

1. Slope-Dependent Transport

[2] There is a long record of work suggesting that soil-mantled hillslopes undergoing "diffusive" soil transport [see *Roering et al.*, 2002a] evolve according to a diffusion-like equation [e.g., *Culling*, 1963, 1965; *Kirkby*, 1967; *Carson and Kirkby*, 1972; *Hirano*, 1975; *Bucknam and Anderson*, 1979; *Nash*, 1980a, 1980b; *Hanks et al.*, 1984; *McKean et al.*, 1993; *Dietrich et al.*, 1995; *Fernandes and Dietrich*, 1997; *Martin and Church*, 1997; *Heimsath et al.*, 1999; *Anderson*, 2002; *Roering et al.*, 2004] when viewed at scales larger than the disturbances producing the transport [*Jyotsna and Haff*, 1997] or the surface roughness associated with vegetation [*Parsons et al.*, 1992; *Abrahams et al.*, 1995; *Bochet et al.*, 2000; *Childs*, 2008]. This diffusion-like equation arises from a statement of soil mass conservation and the assumption of slope-dependent soil transport. Here we explore what gives rise to this slope dependency.

[3] As a point of reference, consider a fixed, global Cartesian *xyz*-coordinate system where the *z*-axis is vertical. Then the most commonly assumed transport formula has the form

$$\mathbf{q}_s = -D\nabla_2\zeta. \tag{1}$$

Here, $\mathbf{q}_s$ is a volumetric flux per unit contour distance [$L^2\ t^{-1}$], $z = \zeta$ denotes the local coordinate of the land surface, D [$L^2\ t^{-1}$] is a diffusion-like coefficient, and $\nabla_2 = \mathbf{i}\partial/\partial x + \mathbf{j}\partial/\partial y$. This and related formulae are sometimes referred to as "geomorphic transport laws" [e.g., *Dietrich et al.*, 2003], and indeed (1) has the form of several classic transport laws, for example, those of *Fourier* [1822], *Fick* [1855], and *Darcy* [1856]: $\mathbf{q}_T = -K_T\nabla T$, $\mathbf{q}_c = -K_c\nabla c_M$ and $\mathbf{q}_h = -K_h\nabla h$, respectively. With $\nabla = \mathbf{i}\partial/\partial x + \mathbf{j}\partial/\partial y + \mathbf{k}\partial/\partial z$, here the flux densities of heat $\mathbf{q}_T$ [$M\ t^{-3}$], mass $\mathbf{q}_c$ [$M\ L^{-2}\ t^{-1}$] and volume $\mathbf{q}_h$ [$L\ t^{-1}$] derive respectively from gradients of temperature T [T], mass concentration c_M [$M\ L^{-3}$], and hydraulic head h [L], as the flux $\mathbf{q}_s$ in (1) derives from a land-surface gradient. The thermal conduc-

[1]Department of Earth and Environmental Sciences and Department of Civil and Environmental Engineering, Vanderbilt University, Nashville, Tennessee, USA.
[2]Division of Earth and Ocean Sciences, Nicholas School of the Environment, Duke University, Durham, North Carolina, USA.
[3]Department of Earth and Planetary Science, University of California, Berkeley, California, USA.
[4]School of Earth and Space Exploration, Arizona State University, Tempe, Arizona, USA.

Copyright 2009 by the American Geophysical Union.
0148-0227/09/2009JF001267$09.00

tivity K_T [M L T^{-1} t^{-3}], kinematic mass diffusivity K_c [L^2 t^{-1}] and hydraulic conductivity K_h [L t^{-1}] are phenomenological coefficients whose units were, on empirical grounds, originally assigned to them to satisfy dimensional homogeneity, as were the units of D in (1). However, aside from fundamental differences in the systems involved, an important practical distinction between these three laws and (1) is that, subsequent to their publication in the 19th century, significant attention has been given to providing a theoretical basis for these classic laws. As a consequence their linear form has a solid theoretical justification and, equally important, the ingredients of the coefficients in these laws have been clearly elucidated. The significance of this latter point is that these coefficients can be related to specific system properties involved in the transport of heat or mass, including properties that might be affected by external factors. In contrast, the form of (1), despite its apparent empirical success, has only a limited theoretical basis; and the diffusion-like coefficient D is mostly a black box, although it must certainly vary with material properties, environmental or climatic variables such as rainfall and temperature, and biological activity [e.g., *Carson and Kirkby*, 1972; *Fernandes and Dietrich*, 1997; *Gabet*, 2000; *Yoo et al.*, 2005].

[4] Following the theoretical work of *Culling* [1960, 1963, 1965], only limited work has been undertaken to describe the details of soil transport with the intent of physically justifying the relation (1), and only a few field-based studies have been undertaken specifically to provide empirical evidence to test the form of (1) [e.g., *Kirkby*, 1967; *Schumm*, 1967; *McKean et al.*, 1993; *Fernandes and Dietrich*, 1997; *Clarke et al.*, 1999; *Gabet*, 2000; *Heimsath et al.*, 2005]. Several models describing soil motion, leading to (1) or to variations on this linear relation, are available. These characterize mechanisms of transport due to expansion and contraction associated with moisture changes or freezing-thawing action [*Davison*, 1889; *Kirkby*, 1967; *Anderson*, 2002], or relate transport to specific biological activity [*Gabet*, 2000; *Yoo et al.*, 2005], or involve continuum rheological hypotheses [e.g., *Kojan*, 1967; *Ahnert*, 1967; *Mitchell et al.*, 1968; *Roering et al.*, 1999] albeit involving a probabilistic basis [e.g., *Roering*, 2004]. Nonetheless, explanations of how the motions of individual soil particles (or particle clumps) collectively contribute to *en masse* motion, possibly leading to the form of (1) or to nonlinear variations, mostly remain heuristic. In addition, little is known about the details of the coefficient D other than it is fundamentally a rate constant [e.g., *Mitchell et al.*, 1968; *Roering*, 2004], and that it qualitatively varies with material properties (e.g., grain size and cohesiveness) and climate based on estimates of D from a variety of environmental settings [e.g., *Carson and Kirkby*, 1972; *Fernandes and Dietrich*, 1997, p. 1309, Table 1]. As described below, for example, $\mathbf{q}_s$ almost certainly depends on the particle size, thickness and vertical porosity structure of a soil as well as the land-surface gradient.

[5] For reference throughout this paper, we note at the outset that the flux $\mathbf{q}_s$ in (1), as a vertically integrated quantity, implicitly contains the local soil thickness h as one of its length scales [*Mudd and Furbish*, 2004; *Paola and Voller*, 2005; *Heimsath et al.*, 2005]. This recommends an altered version of (1), namely [*Furbish and Fagherazzi*, 2001; *Furbish*, 2003; *Mudd and Furbish*, 2004; *Heimsath et al.*, 2005]

$$\mathbf{q}_s = h\overline{\mathbf{q}} = -D\nabla_2\zeta. \tag{2}$$

Here, $\overline{\mathbf{q}} = \mathbf{i}\overline{q}_x + \mathbf{j}\overline{q}_y$ [L t^{-1}] is the vertically averaged volumetric flux density. Namely,

$$\overline{q}_x = \frac{1}{h}\int_\eta^\zeta q_x \mathrm{d}z \quad \text{and} \quad \overline{q}_y = \frac{1}{h}\int_\eta^\zeta q_y \mathrm{d}z, \tag{3}$$

where q_x and q_y [L t^{-1}] are local volumetric flux densities (see sections 2.2 and 2.4), and $h = \zeta - \eta$, where η denotes the base of the active soil thickness. The significance of the relation between (1) and (2) is elaborated below.

[6] Herein we examine how soil particle motions collectively contribute to *en masse* motion, and possibly lead to the form of (1) or (2). Our objective is to pry open the "black box" of transport as articulated by *Dietrich et al.* [2003]. We illustrate that, at least for certain biomechanically driven particle motions, a slope-dependent transport relation, as in (2), obtains from a balance between particle fluxes that tend to loft a soil and the gravitational settling of particles into available pore space. The analysis leads to a kinematic description of the ingredients of the diffusion-like coefficient D. In turn, this leads to a nonlinear transport formula wherein the vertically integrated flux, $\mathbf{q}_s = h\overline{\mathbf{q}}$, is proportional to the "depth-slope product," an idea first suggested by *Ahnert* [1967] but only recently supported by field evidence [*Anderson*, 2002; *Heimsath et al.*, 2005; *Yoo et al.*, 2007].

[7] The focus of this paper is on transport associated with biomechanical mixing and similar processes that involve intermittent soil dilation. Biomechanically induced particle motions are complex, and depend on the specific biota involved as well as on local soil conditions. Faced with this complexity, we purposefully avoid, for now, a formulation of particle motions that is based on a purely mechanistic viewpoint. Rather, our approach combines elements of statistical mechanics and kinematics. This provides a framework for tractably describing particle motions, but the results of the analysis are at a kinematic (rather than dynamic) level. Nonetheless, the analysis provides important insights into ingredients of slope-dependent transport formulae. The main parts of the analysis include the following: (1) a brief conceptual description of soil particle motions (section 2.1); (2) a description of the distinction between "flux density" and particle "transport speed" (section 2.2); (3) a formalization of this distinction based on specialized forms of the Master equation and the Fokker-Planck equation adapted to soil particle motions (sections 2.3 and 2.4); (4) a description of the "mean free path" of passively settling particles (section 2.5); (5) a balancing of fluxes that tend to loft soil particles with a flux due to gravitational settling, leading to a slope-dependent transport relation and a statistical description of the diffusion-like coefficient (section 3); (6) a formulation of a nonlinear "depth-slope" transport relation (section 4); and (7) a

description of field-based evidence for a nonlinear relation (section 5).

2. Soil Particle Motions and Transport

2.1. Modes of Motion

[8] Reminiscent of the early work of *Culling* [1963, 1981], we envision the *en masse* motion of a soil as arising from the collective quasi-random motions of soil particles and particle clumps, where the overall motion involves a net downward component that is gravitationally driven. With biomechanically driven creep, we further envision that particles generally undergo two types of motion: scattering motions and systematic settling motions. (Herein we use the term "creep," for simplicity, to denote *en masse* motion without causal connotation.)

[9] Scattering motions are directionally quasi-random, and represent the collection of particle displacements that are independent of the gravitational field. Such motions are "active" in the sense that they are forced by biological activity, for example, involving displacements by root growth or via ingestion and movement by worms, including movement to the surface [e.g., *Covey*, 2008]. These motions thus may be associated mostly with bioturbation, as in the conceptualization of biomechanical mixing of soil particles suggested by *Heimsath et al.* [2002] and *Kaste et al.* [2007], but they may also arise from other mechanisms whose effect is directionally quasi-random. For example, the zig-zag motions associated with such things as frost heave or wetting-drying cycles [*Kirkby*, 1967; *Anderson*, 2002], and the acoustically excited dilational motions in the experiments of *Roering et al.* [2001] and *Roering* [2004], to some extent may be mimicked by a quasi-random model [*Furbish et al.*, 2008]. The magnitudes of scattering motions may depend on particle sizes and porosity, but also on details of the processes that activate the particles. Scattering motions are responsible for overall soil dilation or lofting, and, as described below, may involve both advective and diffusive parts.

[10] Gravitational settling, in contrast, is unidirectional, and refers to the dislodgment or detachment of a particle from its neighbors, whence the particle settles downward into open pore space. Settling motions are thus "passive." Simple examples include the settling of particles that detach from the wall of an animal burrow or root hole following decay of the root, and the eventual collapse of burrows and root holes. Settling may be indirectly associated with scattering motions inasmuch as these contribute to dislodging of particles which then settle. Other settling motions also are directionally systematic and may involve, for example, downward motions of small particles temporarily suspended within percolating water. The magnitudes of settling motions depend on the availability and size of local pore spaces into which particles can move, a simple but far reaching idea first articulated by *Culling* [1963, 1965, 1981]. Settling motions, although directionally systematic, possess a quasi-random quality and therefore may involve both advective and diffusive parts.

[11] We note that because not all possible modes of biomechanically driven particle motions are necessarily faithfully mimicked by a quasi-random model, for example, the "long-distance" transport of particles associated with large rodents and tree-throw, details of the formulation below are certainly imperfect. Nonetheless, we emphasize that a statistical approach, despite its imperfections, represents an important step forward, as it highlights basic probabilistic ingredients of the problem. We also emphasize the importance of settling motions, which are geometrically and mechanically simple. Details of scattering motions, which generally are more complex, have a less critical role, so the analysis is inherently forgiving of any sins of omission or commission in our treatment of these motions. The analysis contains ingredients that are similar to the "rate process" formulation of *Roering* [2004], notably the idea that particle displacement distances are fundamentally probabilistic. We also aim, as proof-of-concept, at qualitatively reproducing the creep displacement profiles compiled by *Roering* [2004, Figure 1] which show a characteristic exponential-like decline with depth.

2.2. Flux Density Versus Particle Speed

[12] The local (particle) volumetric flux density, denoted by $\mathbf{q} = \mathbf{i}q_x + \mathbf{j}q_y + \mathbf{k}q_z$ [L t^{-1}], is somewhat analogous to the "specific discharge" $\mathbf{q}_h$ in the theory of porous media flows. As such, $\mathbf{q}$ does not generally represent the transport speed of soil particles, despite its units of velocity. (Ambiguity on this point exists in the literature.) There are three essential reasons for this. First, individual particle motions may be complex; particles at any instant move in different directions and at different speeds. Second, at any instant only a subset of particles is undergoing motion; in fact, in many geological situations most particles remain at rest during any small interval of time τ. Third, because $\mathbf{q}$ is a particle volume per unit area per unit time, porosity must be taken into account to determine particle speed.

[13] Consider (for simplicity) a cubic particle with edge b that is moving with speed u through an elementary plane segment A (Figure 1). During a small interval τ the particle moves a distance $\delta x = u\tau$. The small volume of particle passing through the plane during τ is $b^2\delta x = b^2 u\tau$. The (particle) volumetric flux is $b^2\delta x/\tau = b^2 u$, and the volumetric flux density is $b^2\delta x/A\tau = b^2 u/A$. Thus the flux density differs from the particle speed u by a factor of b^2/A.

[14] More generally, consider a large number of cubic particles, each with edge b; some are at rest and some are moving with different velocities, both positive and negative, near and through A. The particles have at any instant the volumetric concentration c, defined as the volume of particles per unit total (sampling) volume, or by $c = 1 - \varphi$, where φ is the porosity. Assuming the particles are quasi-randomly positioned at any instant, their volumetric concentration is equivalent to their areal concentration, defined here by the cross-sectional area of particles that intersect A per area A. Thus, if N particles instantaneously intersect A, then $c = Nb^2/A$, or the specific particle area $b^2/A = c/N$. In addition, let a denote the probability that a particle is in motion. Then a total of aN particles which intersect A are in motion. Following the development above, if the volumetric flux of a single particle moving with speed u_i through A is $b^2 u_i$, then the (total) volumetric flux density is

$$\frac{b^2}{A}\sum_{i=1}^{N} u_i = \frac{b^2}{A}\sum_{i=1}^{N} u_i[1 - H_1(u_i)H_1(-u_i)] \qquad (4)$$

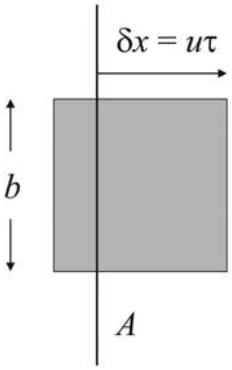

Figure 1. Definition diagram for volumetric flux of idealized cubic particle passing through elementary plane segment A.

or

$$\frac{c}{N}\sum_{i=1}^{N} u_i = \frac{c}{N}\sum_{i=1}^{N} u_i[1 - H_1(u_i)H_1(-u_i)], \tag{5}$$

where the left side is a sum over all N particles, and, with H_1 denoting the Heaviside step function with $H_1(0) \equiv 1$, the right side sums only aN active particles. Multiplying the right side of (5) by a/a, it follows that the flux density is

$$c\overline{u}_A = ac\overline{u}_a, \tag{6}$$

where $\overline{u}_A$ is the average speed of all particles, active and inactive, and $\overline{u}_a$ is the average speed of active particles. It also follows that $\overline{u}_A = a\overline{u}_a$, which is a "virtual speed" of particle motions. Thus, both the flux density and the particle transport speed may be defined in terms of either all (active and inactive) particles, or just active particles.

[15] In turn, the mass flux density through A is $\rho_p c\overline{u}_A$ [M L^{-2} t^{-1}], where ρ_p is the particle density. Moreover, it is common to define the mass flux density as $q_b = \rho_b\overline{u}$ [M L^{-2} t^{-1}], where ρ_b is the soil bulk density and $\overline{u}$ is a characteristic speed. By definition $c = \rho_b/\rho_p$, which means that $\overline{u}$ must be interpreted as the virtual speed, $\overline{u}_A$, rather than the active (actual) particle speed, $\overline{u}_a$. That is, $q_b = \rho_b\overline{u}_A$ or $q_b = \rho_b a\overline{u}_a$. Moreover, whereas the virtual speed $\overline{u}_A = |\mathbf{q}|/c$, the active particle speed $\overline{u}_a = |\mathbf{q}|/ac$. We generalize these ideas next, showing that diffusive-like motions also must be considered [*Culling*, 1981] in defining the local flux density $\mathbf{q}$.

2.3. Master and Fokker-Planck Equations

[16] To describe how the motions of soil particles collectively contribute to the flux density $\mathbf{q}$, we initially consider the probabilistic motion of an individual particle, then generalize the formulation for the situation involving many particles. The centerpiece of the formulation is the Master equation (ME), thus named in the field of statistical mechanics because of its importance in formulating laws of conservation. The objective in presenting this formulation is to illustrate how the flux includes both advective and diffusive parts, a result that is particularly important in characterizing the mixing of soil constituents, including distinct particle fractions (such as specific size or mineral fractions, seeds, or debitage), or elements and compounds adsorbed to particles [e.g., *Kaste et al.*, 2007; *Covey*, 2008], although we then simplify the analysis in focusing on the advective part of settling motions.

[17] Suppose that a particle moves within a Cartesian xyz-coordinate system by means of a series of uneven steps, and that successive steps are Markovian in character. In the context of soils, this means that the particle alternates between states of motion and rest, and details of the motion (e.g., variations in speed) may be neglected. We also assume that the length of each step is unaffected by the previous step.

[18] Let $f(\mathbf{x}, t)$ denote the probability density function associated with particle position $\mathbf{x} = (x, y, z)$. That is, $f(\mathbf{x}, t)\mathrm{d}\mathbf{x}$ is the probability that a particle is within the small interval $\mathbf{x}$ to $\mathbf{x} + \mathrm{d}\mathbf{x}$ at time t. The function $f(\mathbf{x}, t)$ satisfies the condition

$$\int_{-\infty}^{\infty} f(\mathbf{x}, t)\mathrm{d}\mathbf{x} = 1, \tag{7}$$

where it is understood that the integration is over a three-dimensional domain. At any instant, only a proportion of the particles in a soil may be in motion. Thus, let $a(\mathbf{x}, t)$ denote the probability that a particle at position $\mathbf{x}$ is active at time t and undergoes motion during a small interval $\mathrm{d}t$. The probability that a particle remains at rest during $\mathrm{d}t$ is $1 - a(\mathbf{x}, t)$. It also is useful to explicitly take into account different possible modes of particle motion. Specifically, let $M_j(\mathbf{x}, t)$ denote the probability associated with a particular mode j, where $j = 1, 2, \ldots$, satisfying the condition that

$$\sum\nolimits_j M_j(\mathbf{x}, t) = 1, \tag{8}$$

which applies to particles in motion, not those at rest. As described below it is convenient in the present case to specify that a particle motion is either a scattering motion, with probability M_1, or a gravitational settling motion, with probability M_2, such that $M_1 + M_2 = 1$.

[19] The Master equation [*Risken*, 1984] may be written as (Appendix A)

$$\frac{\partial f(\mathbf{x}, t)}{\partial t} = \int_{-\infty}^{\infty} f(\mathbf{x}', t)a(\mathbf{x}', t)\sum\nolimits_j M_j(\mathbf{x}', t)V_j(\mathbf{x}, \mathbf{x}', t). \tag{9}$$

Here, $V_j(\mathbf{x}, \mathbf{x}', t)$ is defined by

$$V_j(\mathbf{x}, \mathbf{x}', t) = \lim_{\mathrm{d}t \to 0} \frac{W_j(\mathbf{x}, t + \mathrm{d}t|\mathbf{x}', t) - \delta(\mathbf{x} - \mathbf{x}')}{\mathrm{d}t}, \tag{10}$$

where W_j is the conditional probability that a particle involving mode j is at $\mathbf{x}$ at time $t + \mathrm{d}t$ given that it was at $\mathbf{x}'$ at time t, and δ is the Dirac function. The right side of (9) in effect describes the difference in the rate at which grains arrive at $\mathbf{x}$ from all other positions $\mathbf{x}'$ and the rate at which grains leave position $\mathbf{x}$. The probability that a particle moves from position $\mathbf{x}'$ to $\mathbf{x}$ during $\mathrm{d}t$ is identical to the probability that, starting from position $\mathbf{x} - \mathbf{r}$, it undergoes a displacement equal to $\mathbf{r} = \mathbf{x} - \mathbf{x}'$ during $\mathrm{d}t$. This means that the function W_j can be interpreted as a local probability density of particle displacement distances $\mathbf{r}$, in which

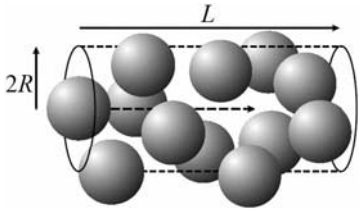

Figure 2. Definition diagram for calculating mean free path l.

case (9) has the differential form [*Chandrasekhar*, 1943; *Risken*, 1984] (Appendix B)

$$\frac{\partial f(\mathbf{x},t)}{\partial t} = -\frac{\partial}{\partial \mathbf{x}}\left(fa\sum\nolimits_j M_j m_{1j}\right) + \frac{1}{2}\frac{\partial^2}{\partial \mathbf{x}^2}\left(fa\sum\nolimits_j M_j m_{2j}\right) - \ldots, \tag{11}$$

where m_{ij} is the ith moment of W_j in the limit of $\mathrm{d}t \to 0$, as in (10) (Appendix B). Truncated at second order (11) is the Fokker-Planck (FP) equation, where m_{1j} and m_{2j} are interpreted, respectively, as the grain drift velocity $\mathbf{u}_j$ and the diffusion (or dispersion) coefficient tensor $\mathbf{D}_j$. Related formulations involving fractional derivatives [*Schumer et al.*, 2009] open the possibility of describing anomalous diffusion/dispersion, a well studied topic in physics, but emerging only recently as a topic of study in porous media transport [*Benson et al.*, 2000a, 2000b, 2001] and sediment transport [*Nikora et al.*, 2002; D. N. Bradley et al., Anomalous dispersion in a sand-bed river, submitted to *Journal of Geophysical Research*, 2009; V. Ganti et al., Normal and anomalous dispersion of gravel tracer particles in rivers, submitted to *Journal of Geophysical Research*, 2009]. Nonetheless, for the purpose herein of describing ingredients of the flux density $\mathbf{q}$, it suffices to work with the classic advection-dispersion (FP) equation.

[20] As elaborated below, the novelty of (9) and (11) resides in the explicit appearance of the particle activity probability a and the modes M_j, which do not appear in classic formulations (Appendix A). This directly connects intermittent particle motions to their sources: biological activity and gravity. (Setting $a = 1$ with $j = 1$ retrieves the classic ME and FP equation for continuously moving particles.) The formulation also explicitly separates this activity from the "mechanics" of grain motions, which are embedded within the moments m_{ij}.

2.4. Particle Flux Densities

[21] We hereafter make several simplifying assumptions and definitions. First, because we intend only to provide a kinematic description of transport we assume that the particles have approximately the same size and shape. Second, we consider only two-dimensional transport parallel to x and z so that $m_{1j} = \mathbf{u}_j = \mathbf{i}u_j + \mathbf{k}w_j$. Third, we assume that the diffusion-like coefficient is a scalar quantity, namely $m_{2j} = D_j$, which is equivalent to assuming that D_j is isotropic. Fourth, we consider only the two modes of motion described in section 2.1, denoting scattering motions by $j = 1$ and settling motions by $j = 2$. With these assumptions the probability f in (11) can be mapped directly to particle concentration c, the volume of particles per unit total volume. Then, c and f differ only by a constant (Appendix B) and (11) truncated at second order becomes

$$\frac{\partial c(x,z,t)}{\partial t} = -\frac{\partial}{\partial x}\left(c\,a\sum\nolimits_j M_j u_j\right) - \frac{\partial}{\partial z}\left(c\,a\sum\nolimits_j M_j w_j\right) + \frac{1}{2}\frac{\partial^2}{\partial x^2}\left(c\,a\sum\nolimits_j M_j D_j\right) + \frac{1}{2}\frac{\partial^2}{\partial z^2}\left(c\,a\sum\nolimits_j M_j D_j\right). \tag{12}$$

By definition in this two-dimensional case,

$$\frac{\partial c}{\partial t} = -\frac{\partial q_x}{\partial x} - \frac{\partial q_y}{\partial z}. \tag{13}$$

Comparing (13) with (12), it follows that the volumetric flux density components, q_x and q_z, are

$$q_x = c\,a\,M_1 u_1 - \frac{1}{2}\frac{\partial}{\partial x}(c\,a\,M_1 D_1) + c\,a\,M_2 u_2 - \frac{1}{2}\frac{\partial}{\partial x}(c\,a\,M_2 D_2) \tag{14}$$

and

$$q_z = c\,a\,M_1 w_1 - \frac{1}{2}\frac{\partial}{\partial z}(c\,a\,M_1 D_1) + c\,a\,M_2 w_2 - \frac{1}{2}\frac{\partial}{\partial z}(c\,a\,M_2 D_2), \tag{15}$$

wherein it is further apparent that q_x and q_z consist of sums of scattering and settling flux densities; that is $q_x = q_{x1} + q_{x2}$ and $q_z = q_{z1} + q_{z2}$.

[22] Momentarily returning to (12), note that D_j is formally inside the second derivatives, which means that it is more appropriate to think of this quantity as a variable than as a coefficient. This result is at odds with formulations that directly embed a Fick-like (or Fourier-like) law inside a statement of conservation like (13), wherein D_j then appears inside one, but not both, of the derivatives. In a local formulation like that presented here, D_j belongs either entirely inside, or entirely outside, the second derivatives, a decision that must rest on a physical argument rather than a mathematical one.

[23] As described below (section 3), the details of the (bio)mechanics of particle motions are contained in the quantities a, u_j, w_j, M_j and D_j. Before using the results of this section to examine the flux relation (2), however, we require one more ingredient, the mean free path as applied to settling motions.

2.5. Mean Free Path

[24] The mean free path l of a soil particle is obtained from a straightforward geometrical argument that is similar to that used in the kinetic theory of gases [e.g., *Jeans*, 1960]. Envision a sphere with radius R that translates a distance L within a mixture of similar, quasi-randomly arranged spheres with density N_V [number L^{-3}] (Figure 2). The encompassed volume that involves particle "collisions" during this motion is $4\pi R^2 L$, so the number of collisions N is

$$N = 4\pi R^2 L N_V. \tag{16}$$

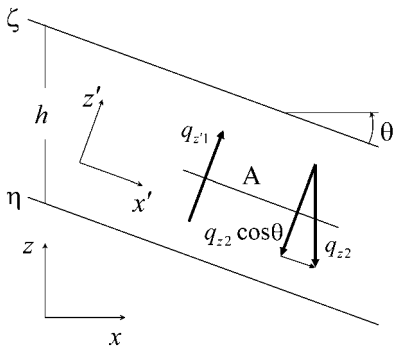

Figure 3. Definition diagram for fluxes across elementary plane segment A within uniform active soil involving steady creep.

In turn, letting N_{Vm} denote a natural consolidated (maximum) volumetric density, it follows that the maximum number of collisions possible is $N_m = 4\pi R^2 L N_{Vm}$. The average spacing (measured parallel to the direction of L) between particles is $L/N = 1/4\pi R^2 N_V$, and the spacing between particles at the consolidated density is $L/N_m = 1/4\pi R^2 N_{Vm}$. The mean free path l is equal to the spacing between particles in excess of that at the consolidated density. That is,

$$l = \frac{1}{4\pi R^2 N_V} - \frac{1}{4\pi R^2 N_{Vm}}. \tag{17}$$

It is straightforward to demonstrate that $N_V = 3c/4\pi R^3$ and N_{Vm} $N_{Vm} = 3c_m/4\pi R^3$, whereupon substituting these expressions into (17) leads to

$$l \sim \frac{k_A R}{c_m}\left(\frac{c_m}{c} - 1\right), \tag{18}$$

where k_A is a dimensionless coefficient (equal to 1/3 in the case of spherical particles), and c_m is a natural consolidated concentration. Although this formulation of l can be generalized for mixtures of particle sizes [*Strong and Furbish*, 1999], including particle clumps, the use of a single size suffices here.

[25] The formulation above gives values of l that are on the order of a particle diameter or smaller for typical values of c and c_m when viewed at a scale that does not include macropores. The length L therefore must be envisioned as being large enough to fully sample the soil porosity structure, including macropores; and the mean free path l is an average for what must be an exponential-like (or possibly even heavy-tailed) distribution of free path motions that include, in the case of settling motions, distances comparable to the size of macropores.

3. Slope-Dependent Transport and the Diffusion-Like Coefficient

3.1. Slope-Dependent Transport

[26] The slope-dependent form of (2), and a kinematic expression for the diffusion-like coefficient D in (2), can be obtained assuming that the collective quasi-random motions of soil particles involve scattering motions and gravitational settling motions (section 2.1). Consider a planar hillslope inclined at an angle θ, with uniform active soil thickness $h = \zeta - \eta$ as measured in the vertical direction, not perpendicular to the surface, and involving steady creep (Figure 3). In this situation, the effect of bioturbation is to loft the soil column such that the particle concentration generally decreases toward the surface, whereas particle concentration gradients and flux gradients parallel to the surface vanish. In particular, momentarily consider an inclined $x'z'$-coordinate system whose x'-axis is parallel to the slope (Figure 3). Then in the steady case (with $\partial c/\partial t = 0$)

$$\frac{\partial q_{x'}}{\partial x'} + \frac{\partial q_{z'}}{\partial z'} = 0. \tag{19}$$

The uniform condition requires that $\partial q_{x'}/\partial x' = 0$, $\partial q_{z'}/\partial z' = 0$ and $q_{z'} = 0$, but leaves open the possibility that $\partial q_{x'}/\partial z'$ is not zero, i.e., $q_{x'} = q_{x'}(z')$. So, across any elementary plane segment A parallel to the soil surface (Figure 3), the net normal flux density must equal zero.

[27] Because gradients in the particle concentration c and the activity probability a parallel to x' are zero, no net diffusive scattering flux parallel to x' occurs. If we also momentarily assume that no slope-parallel bias in these directionally quasi-random motions occurs (but see section 6), then there is no net advective scattering flux density parallel to x'. Thus, $q_{x'1} = 0$, so $q_{x'} = q_{x'2}$, where $q_{x'2}$ is an apparent flux density related to settling. In contrast, the flux density

$$q_{z'} = q_{z'1} + q_{z2}\cos\theta = 0, \tag{20}$$

which indicates that the scattering flux normal to A, $q_{z'1}$, is balanced by the component of the (vertical) settling flux normal to A, $q_{z2}\cos\theta$ (Figure 3). In turn, the horizontal flux density $q_x = q_{z'1}\sin\theta = -q_{z2}\cos\theta\sin\theta$. (Or, with the apparent flux density $q_{x'2} = -q_{z2}\sin\theta$, the horizontal component $q_x = q_{x'2}\cos\theta = -q_{z2}\cos\theta\sin\theta$.) This may be written as

$$q_x = q_{z2}\cos^2\theta\frac{\partial\zeta}{\partial x}. \tag{21}$$

Using the definition of the vertically integrated flux given by (2) and (3),

$$h\overline{q}_x = \int_\eta^\zeta q_x \mathrm{d}z = \left(\int_\eta^\zeta q_{z2}\mathrm{d}z\right)\cos^2\theta\frac{\partial\zeta}{\partial x}. \tag{22}$$

This, without further ado, describes a slope dependence in the transport arising from a balance of scattering and settling fluxes, going beyond heuristic arguments for such a dependence. But with further ado, we can obtain a kinematic description of the diffusion-like coefficient D in (2) by specifying the flux density q_{z2} in (22) as follows.

3.2. Diffusion-Like Coefficient

[28] According to (15),

$$q_{z2} = c\,a\,M_2 w_2 - \frac{1}{2}\frac{\partial}{\partial z}(c\,a\,M_2 D_2). \tag{23}$$

Starting with w_2 and D_2 in (23) and letting κ denote the vertical component of the particle displacement distance **r**, these quantities are formally defined as (Appendix B)

$$w_2(x,z,t) = \lim_{\mathrm{d}t\to 0} \frac{1}{\mathrm{d}t} \int_{-\infty}^{\infty} \kappa U_2(z,\kappa;t,\mathrm{d}t)\mathrm{d}\kappa \quad \text{and}$$
$$D_2(x,z,t) = \lim_{\mathrm{d}t\to 0} \frac{1}{\mathrm{d}t} \int_{-\infty}^{\infty} \kappa^2 U_2(z,\kappa;t,\mathrm{d}t)\mathrm{d}\kappa, \tag{24}$$

where U_2 is the probability density of displacements κ. Because settling motions are passive and therefore depend on the availability and size of local pore spaces into which particles can move (section 2.1 [*Culling*, 1963, 1965, 1981]), we may assume that the average $\overline{\kappa}$ of the probability density U_2 is proportional to the mean free path l (section 2.5). That is $\overline{\kappa} = k_2 l$, where k_2 is a coefficient of order unity. Letting τ denote the mean free time involved in particle settling over the distance $k_2 l$, consistent with the assumption of Markov-like behavior (section 2.3), then to a good approximation

$$w_2(x,z,t) \sim \frac{\overline{\kappa}}{\tau} \sim k_2 \frac{l}{\tau} \quad \text{and} \quad D_2(x,z,t) \sim \frac{\overline{\kappa}^2}{\tau} \sim k_2^2 \frac{l^2}{\tau}. \tag{25}$$

(Note that this is similar to the idea of *Roering* [2004], that the displacement of a particle is a random variable obtained from a distribution of excitation heights.)

[29] A simple scaling analysis (Appendix C) indicates that the diffusive term in (23) can be neglected when the average settling motion $\overline{\kappa} \sim k_2 l$ close to the soil surface is significantly less than the active soil thickness h. Then, for passively settling particles, we may also incorporate (18) into (24) to give

$$w_2 \sim -\frac{1}{\tau}\frac{kR}{c_m}\left(\frac{c_m}{c} - 1\right), \tag{26}$$

where $k = k_A k_2$ and the negative sign is required by the definition of settling.

[30] Turning to the probability M_2 in (23), for physical reasons $M_2 \to 0$ when $c \to c_m$, and $M_2 \to 1$ when $c \to 0$. That is, a passive settling motion cannot occur in the absence of available pore space, and settling must occur at exceedingly low concentrations. It is therefore reasonable to assume that

$$M_2 = 1 - \frac{c}{c_m}. \tag{27}$$

Because $M_1 + M_2 = 1$, this means that $M_1 = c/c_m$. Thus, if a particle motion occurs when $c \to c_m$, it must be (bio)mechanical. Whereas the behavior of M_2 at the limits stated above is physically correct, uncertainty arises between these limits. (The variation in M_2 with c is not necessarily linear.) Nonetheless, (27) certainly captures the lowest-order structure of M_2, which suffices for our aim at a kinematic description of q_{z2}.

[31] Substituting (26) and (27) into (23) and neglecting the diffusive term

$$q_{z2} = -\frac{akR}{\tau}\left(1 - \frac{c}{c_m}\right)^2. \tag{28}$$

The activity probability a may now be interpreted as follows. Let $N_a(z)$ [t^{-1}] denote the number of times a particle is activated per unit time. Then $N_a T$ is the number of activations during T and $N_a T\tau$ is the time that the particles are actually in motion during T. The probability a may then be defined as $a = N_a T\tau/T = N_a\tau$. Substituting this into (28), and the resulting expression into (21)

$$q_x = -kRN_a\left(1 - \frac{c}{c_m}\right)^2 \cos^2\theta \frac{\partial\zeta}{\partial x}. \tag{29}$$

In turn, substituting this into (22) and evaluating the integral leads to

$$h\overline{q}_x = -k\,R\,h\overline{N_a\left(1 - \frac{c}{c_m}\right)^2}\cos^2\theta\frac{\partial\zeta}{\partial x}, \tag{30}$$

where the overbar denotes vertical averaging. This has the form of (2), where the diffusion-like coefficient D is

$$D = k\,R\,h\overline{N_a\left(1 - \frac{c}{c_m}\right)^2}\cos^2\theta. \tag{31}$$

The analysis thus suggests that D contains the active soil thickness h as one of its fundamental length scales. We defer further description of (29), (30), and (31) to section 4.

4. Nonlinear Transport Formula

4.1. Depth-Slope Product

[32] The appearance of the active soil thickness h on the right side of (30) immediately suggests that this can be reformulated as

$$h\overline{q}_x = -D^* h\cos^2\theta\frac{\partial\zeta}{\partial x}, \tag{32}$$

where D^* [$\mathrm{L\ t}^{-1}$] is:

$$D^* = kR\overline{N_a\left(1 - \frac{c}{c_m}\right)^2}. \tag{33}$$

Thus, the vertically integrated flux $h\overline{q}_x$ is proportional to the depth-slope product, with geometrical factor $\cos^2\theta$. Dividing (32) by h gives

$$\overline{q}_x = -D^*\cos^2\theta\frac{\partial\zeta}{\partial x}, \tag{34}$$

which implies that the vertically averaged flux density $\overline{q}_x$ (as opposed to the vertically integrated flux) is proportional to the slope, with geometrical factor $\cos^2\theta$.

[33] The coefficient D^* involves a characteristic particle size R, the vertical concentration (porosity) structure $c(z)$, and the rate of particle activation as a function of depth $N_a(z)$. It is a quasi-local coefficient, as it involves the vertical integration of particle activity and concentration. The quantity $kR(1 - c/c_m)^2$ [L] in effect characterizes the

magnitude of settling motions as determined by the availability and size of local pore spaces into which particles can move. The quantity N_a [t^{-1}] in effect characterizes the frequency with which particles are activated in relation to biological activity. Thus, D^* represents the magnitude-frequency product of particle motions, and it thereby sets the rate constant of the transport process. Similar remarks pertain to D in (31), although this coefficient also includes the active soil thickness h.

4.2. Local Transport

[34] Returning momentarily to (29), this expression suggests that the local flux density $q_x(z)$ is a function of the activity $N_a(z)$ and concentration $c(z)$. We can obtain insight into q_x by heuristically specifying the vertical structure of N_a and c. Specifically, suppose that

$$N_a = N_{a\zeta} e^{-\psi/\alpha} \quad \text{and} \tag{35}$$

$$c = c_m - (c_m - c_\zeta) e^{-\psi/\beta}, \tag{36}$$

where $N_{a\zeta}$ and c_ζ are the values of N_a and c at the soil surface, and α and β are length scales that characterize the rates at which N_a and c change with depth $\psi = \zeta - z$ beneath the surface. Thus, for given values of $N_{a\zeta}$ and c_ζ, small values of α and β imply rapid changes with depth, and large values of α and β imply relative uniformity with depth. Thus, (35) heuristically describes the situation where biological activity, and thus the particle activation rate, decreases with depth; and (36) describes the situation where particle concentration increases with depth (Figure 4), asymptotically approaching the consolidated concentration c_m, although not necessarily involving a smooth transition at the base of the active soil thickness. Indeed, *Roering* [2008] employs the form of (35) to specify the local density of soil disturbances responsible for transport, analogous to N_a, and appeals to the consistency with depth distributions of root density. Whether this represents a general description of the relevant disturbance signal in a specific environmental setting is an open question; nonetheless, the length scale α is a useful artifice to specify whether disturbances are concentrated near the surface or distributed more uniformly with depth.

[35] Substituting (35) and (36) into (29), then for given slope the flux density $q_x(z)$ generally is largest at the soil surface, declining exponentially with depth (Figure 5), entirely consistent with displacement profiles for various creep mechanisms compiled by *Roering* [2004, Figure 1]. With small α or β relative to the active soil thickness h, transport is concentrated near the soil surface; with increasing α or β relative to h, transport becomes increasingly uniform with depth. These displacement profiles reflect the combination of decreasing particle activity with depth, and a decline in the magnitude of particle motions with decreasing availability of pore space as concentration increases with depth. We elaborate on these points below (section 5.3) with reference to the bulk density data in Figure 4.

[36] We can also use (35) and (36) to heuristically examine the behavior of the coefficient D^* in (33). Substituting (35) and (36) into (33), evaluating the vertical average over h, and expanding the result as an exponential series

$$D^* = kRN_{a\zeta}\left(1 - \frac{c_\zeta}{c_m}\right)^2 \cdot \left[1 - \frac{1}{2}\left(\frac{1}{\alpha} + \frac{2}{\beta}\right)h + \frac{1}{6}\left(\frac{1}{\alpha} + \frac{2}{\beta}\right)^2 h^2 - \ldots\right]. \tag{37}$$

We see to leading order that D^* depends on the reference (surface) values $N_{a\zeta}$ and c_ζ. Inasmuch as α and β are independent of the active soil thickness h, then for large α and β relative to h (such that N_a and c become increasingly uniform over depth [*Heimsath et al.*, 2002]), D^* approaches a constant value, independent of h. With small α or β relative to h, however, D^* is not independent of h. This would introduce to the transport formula (32) additional nonlinearity in h. However, in view of the uncertainty surrounding the settling probability M_2 given by (27), and the heuristic nature of (35) and (36), further clarification of this point requires a full theory of soil creep. We therefore assume for simplicity that D^* is constant, independent of the active soil thickness h, for comparison with field data below.

5. Evidence and Examples

5.1. Analysis of Field Measurements

[37] Analogous to the hypothesis of *McKean et al.* [1993], (30) and (34) in effect represent the hypothesis that the vertically averaged soil flux density (rather than the vertically integrated flux) is proportional to slope, such that the vertically integrated flux is proportional to the product of the active soil thickness and slope, the depth-slope product [*Ahnert*, 1967; *Heimsath et al.*, 2005; *Yoo et al.*, 2007]. This is consistent with the idea that the basic mechanism of creep, whether due to biomechanically-driven particle motions, expansion and contraction of clay particles and peds, or otherwise purely mechanical processes, ought to reflect local variations with depth [*Roering*, 2004, 2008], independent of soil thickness. That is, the length scales of particle motions are determined by local processes and soil conditions involved.

[38] At the site described by *McKean et al.* [1993], evidence of bioturbation (e.g., burrowing) exists, but the creeping motion at this site probably is predominantly a shear-like flow associated with wetting, drying and cracking of the clay-rich soil. Estimates of $\overline{q}_x$ and $h\overline{q}_x$, obtained from a formulation involving conservation of cosmogenic isotopes *McKean et al.* [1993], pertain to the situation where it may be assumed that the local soil thickness, vertically averaged soil concentration and vertically averaged ^{10}Be concentration, do not vary significantly with time (although these may vary with position). Specifically, for one-dimensional transport conservation of soil mass requires that

$$\frac{\partial}{\partial x}(h\overline{q}_x) + \frac{\partial}{\partial t}(h\overline{c}) + c_\eta p_\eta = 0, \tag{38}$$

where $\overline{c}$ is the vertically averaged soil concentration, c_η is the concentration at the base of the active soil thickness, and

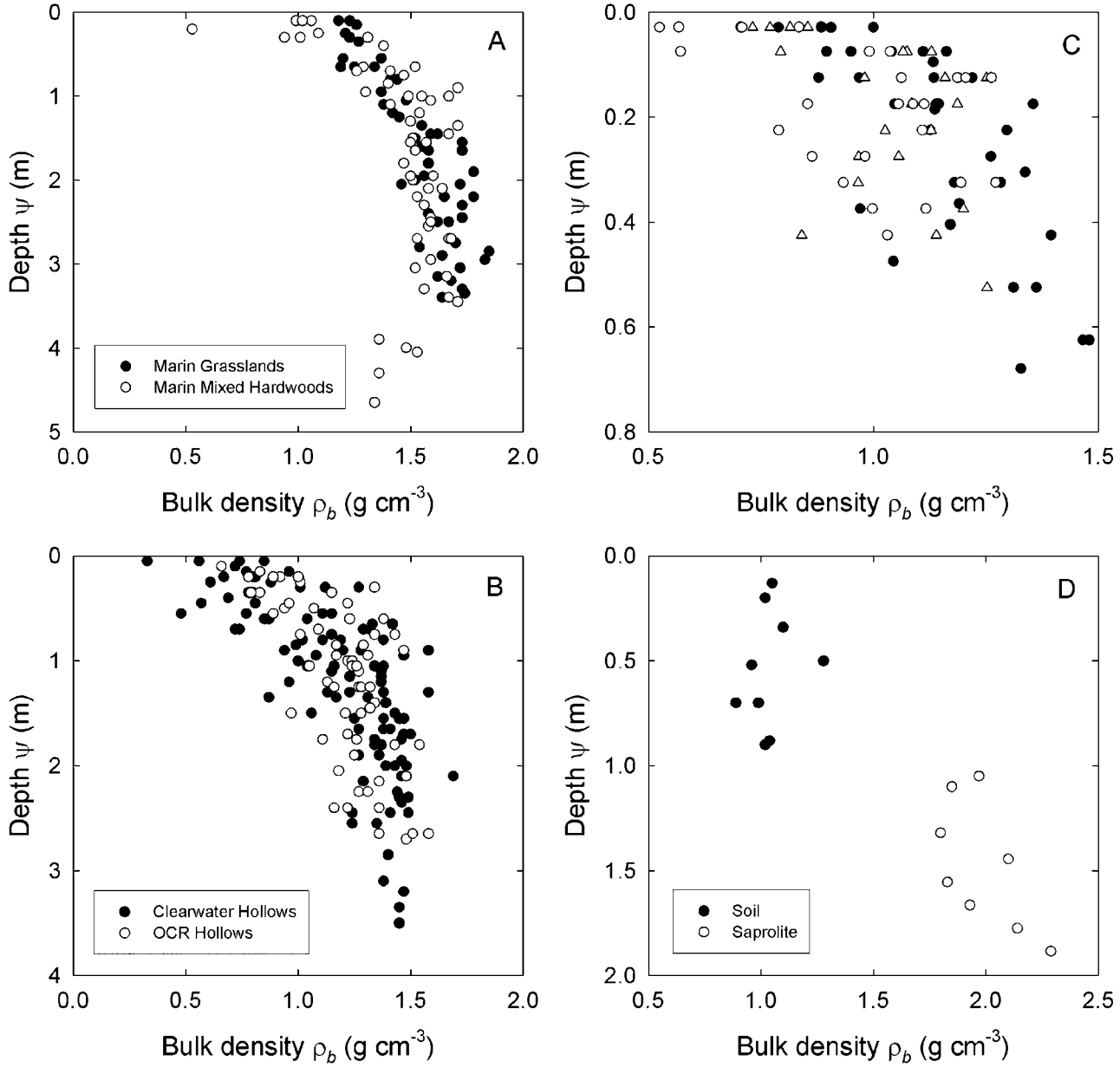

Figure 4. Profiles of soil bulk density ρ_b with depth beneath surface ψ for (a) colluvial fill soils at grassland and mixed hardwood sites in Marin County, California [*Reneau et al.*, 1984, *Reneau and Dietrich*, 1987; *Reneau*, 1988]; (b) forested colluvial fill soils in the Clearwater area, Washington [*Reneau*, 1988; *Reneau et al.*, 1989] and the Oregon Coast Range (OCR) [*Reneau*, 1988; *Reneau and Dietrich*, 1991]; (c) hickory-oak forested soils along three transects (separate symbols) within the Land Between The Lakes national recreation area, Tennessee [*Roseberry and Furbish*, 2008; *Roseberry*, 2009]; and (d) hillslope soils (covered periodically through burn cycles with Bishop pine, grass, and shrubs) at Point Reyes, California. Bulk density increases with depth for Figures 4a–4c but is approximately uniform for Figure 4d with abrupt change at soil-saprolite interface ($\psi \sim 1$ m), apparently because of being well stirred throughout the active profile. Note that with the volumetric concentration $c = \rho_b/\rho_s$, *Reneau* [1988] suggests the bulk density values in Figures 4a and 4b are about 6% less than the true values, and that each datum in Figure 4d is an average of three to five measurements. Uppermost weathered bedrock densities are 2.3 g cm^{-3} at California sites (Figure 4a), 2.2 g cm^{-3} at Clearwater sites (Figure 4b), and 2.03 (sheeted sandstone) and 2.27 g cm^{-3} (unsheeted sandstone) at Oregon Coast Range sites (Figure 4b) [*Reneau*, 1988].

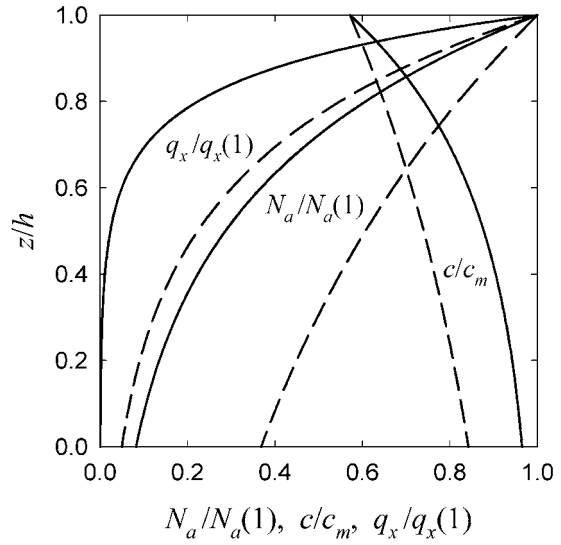

Figure 5. Variations in particle activation N_a, concentration c, and flux density q_x, normalized by surface values and by c_m, over dimensionless depth z/h; $\alpha = \beta = 0.4$ m (solid lines) and $\alpha = \beta = 1$ m (dashed lines).

p_η [L t^{-1}] is the rate of vertical motion of this base. Note that if the base of the active thickness coincides with the soil-saprolite interface and this interface is moving downward, then c_η is the concentration of the saprolite just beneath the interface and p_η is the rate of conversion of saprolite to soil, the "soil production" rate. Otherwise p_η is the rate of entrainment of soil material with concentration c_η into the active thickness (p_η negative), or disentrainment of material from the active thickness (p_η positive). In turn, conservation of atmospherically deposited ^{10}Be requires that

$$\frac{\partial}{\partial x}(h\overline{c_B q_x}) + \frac{\partial}{\partial t}(h\overline{c_B c}) + c_\eta c_{B\eta} p_\eta = \frac{P_B}{\rho_s}, \tag{39}$$

where c_B [M $^{-1}$] is the concentration of ^{10}Be (number of atoms per unit soil mass), $c_{B\eta}$ is the ^{10}Be concentration at the soil-saprolite interface, P_B [L^{-2}] is the ^{10}Be deposition rate per unit area, ρ_s [M L^{-3}] is the particle mineralogical density, and overbars denote vertically averaged quantities.

[39] Integrating (38) and (39) with respect to x,

$$h\overline{q}_x = -\int_0^X \frac{\partial}{\partial t}(h\overline{c})\mathrm{d}x - \int_0^X c_\eta p_\eta \mathrm{d}x \qquad \text{and} \tag{40}$$

$$h\overline{c_B q_x} = -\int_0^X \frac{\partial}{\partial t}(h\overline{c_B c})\mathrm{d}x - \int_0^X c_\eta c_{B\eta} p_\eta \mathrm{d}x + \frac{P_B}{\rho_s}X, \tag{41}$$

where it is assumed that P_B is uniform. The integrals (40) and (41) are evaluated from the divide ($x = 0$ where $h\overline{q}_x = h\overline{c_B q_x} = 0$) to a specified distance X downslope. Applying Leibniz's rule to the first integral quantity in (40),

$$h\overline{q}_x = -X\frac{\partial\langle h\overline{c}\rangle}{\partial t} - \int_0^X c_\eta p_\eta \mathrm{d}x, \tag{42}$$

where $\langle h\overline{c}\rangle$ is spatially averaged over X. If it is assumed that $\langle h\overline{c}\rangle$ does not change significantly over time, then the flux $h\overline{q}_x$ is simply the integral of the soil production rate from $x = 0$ to $x = X$. Conversely, such an estimate of $h\overline{q}_x$ is in error by an amount equal to the second term in (42) if $\langle h\overline{c}\rangle$ is unsteady. Similarly, (41) becomes

$$h\overline{c_B q_x} = -X\frac{\partial\langle h\overline{c_B c}\rangle}{\partial t} - \int_0^X c_\eta c_{B\eta} p_\eta \mathrm{d}x + \frac{P_B}{\rho_s}X. \tag{43}$$

If $\langle h\overline{c_B c}\rangle$ does not change significantly over time, then the flux $h\overline{c_B q_x}$ is obtained from the last two terms in (43) evaluated from $x = 0$ to $x = X$.

[40] A scaling analysis provided by *Heimsath et al.* [2005, Appendix] suggests that the unsteady term in (42) can be neglected if the mean soil residence time, $T_R \sim H/p_\eta$, is much less than the hillslope relaxation time, $T_X \sim X^2/D$ (or $T_X \sim X^2/D^*H$), where H is a characteristic soil thickness, p_η is considered a characteristic (average) rate of soil production, and X is the hillslope length. In effect, if $T_R \ll T_X$, then even with nonuniform soil production, throughput of soil is much faster than transient storage of soil (i.e., $\partial\langle h\overline{c}\rangle/\partial t$) such that production is accommodated almost entirely by the soil flux term. These conditions are more likely to be satisfied away from the bounding channel and on divergent topography [*Heimsath et al.*, 2005]. Similar conclusions pertain to the unsteady term in (43).

[41] Consistent with the analysis of *McKean et al.* [1993] we neglect the unsteady terms in (42) and (43) and further assume that $\overline{c_B q_x} \approx \overline{c_B}\ \overline{q_x}$. Combining the simplified versions of (42) and (43) then gives

$$\frac{P_B X}{\rho_s} = \int_0^X c_{B\eta} c_\eta p_\eta \mathrm{d}x - \overline{c}_B(X)\int_0^X c_\eta p_\eta \mathrm{d}x. \tag{44}$$

Using data from *McKean et al.* [1993] we numerically solve (44) to obtain values of the production p_η, then use (42), neglecting the unsteady term, to obtain values of the flux $h\overline{q}_x$.

[42] Plotting $h\overline{q}_x/\cos^2\theta$ versus slope $S = -\partial\zeta/\partial x$ (Figure 6), with the expectation of a linear relation passing through the origin, is equivalent to testing the hypothesis that the soil flux is proportional to the land-surface slope (modulated by the geometric factor $\cos^2\theta$). Plotting $\overline{q}_x/\cos^2\theta$ versus S (Figure 6), again with the expectation of a linear relation passing through the origin, tests the hypothesis that the vertically averaged flux density is proportional to the slope, such that the soil flux is proportional to the depth-slope product. In view of uncertainty in the data related to the assumption that $\overline{c_B q_x} \approx \overline{c_B q_x}$ as well as field and analytical methods, the data are consistent with either hypothesis. Owing to the small variation in soil thickness at the study site, the data cannot distinguish between these possibilities.

[43] Turning to the data of *Heimsath et al.* [2005], estimates of $h\overline{q}_x$ were obtained using (42) without the unsteady term for three hillslope sites: Tennessee Valley and Point Reyes, California, and Nunnock River, Australia. As described by *Heimsath et al.* [2005], this involved specifying a set of soil "flow lines" defined as being locally normal to elevation contour lines. The "flow tubes" between adjacent flow lines were then divided into increments

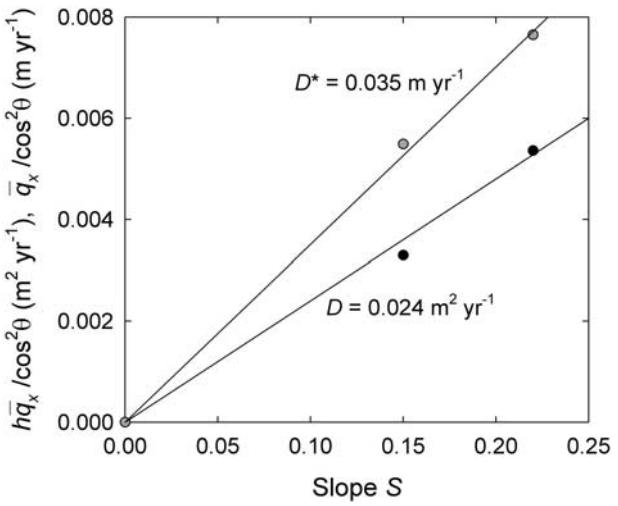

Figure 6. Plot of modified soil flux $h\overline{q}_x/\cos^2\theta$ (black circles) and modified vertically averaged flux $\overline{q}_x/\cos^2\theta$ (gray circles) versus slope S with eye fit estimates of transport coefficient D^* and diffusion-like coefficient D; data taken from *McKean et al.* [1993].

defined by 2-m contour intervals. For each flow tube the average soil thickness h_j for the jth increment was estimated as a Voronoi-polygon-weighted value, namely $h_j = (1/A_j)\sum a_i h_i$, where $A_j = \sum a_i$ is the total area of the interval and a_i is the ith polygon sub-area associated with the soil thickness h_i. The average soil-production rate $p_{\eta j}$ also was estimated as a Voronoi-polygon-weighted value, namely $p_{\eta j} = (P/A_j)\sum a_i \exp(-h_i/\gamma)$, where P is the nominal production rate as h_i approaches zero and γ is a length scale characterizing how quickly the production rate declines with increasing soil thickness. Numerical values of P and γ are provided by *Heimsath et al.* [2005]. The land-surface slope was estimated as an arithmetic average of several finite-difference estimates.

[44] We reproduce here the data for the Nunnock River site, incorporating the geometrical factor $\cos^2\theta$. Plotting $h\overline{q}_x$ versus $S\cos^2\theta$ (Figure 7a), with the expectation of a linear relation passing through the origin, is equivalent to testing the hypothesis that the soil flux is proportional to the land-surface slope (modulated by the geometric factor $\cos^2\theta$). Plotting $h\overline{q}_x$ versus $hS\cos^2\theta$ (Figure 7b), again with the expectation of a linear relation passing through the origin, tests the hypothesis that the soil flux is proportional to the depth-slope product. As described by *Heimsath et al.* [2005], there is the possibility of a spurious correlation between soil flux and slope, as both generally increase downslope. Nonetheless, the data in this case are consistent with the hypothesis that the flux is proportional to the product of slope and active soil thickness.

5.2. Hillslope Profiles

[45] When (32) is substituted into a statement of mass conservation, the factor $\cos^2\theta$ contributes a nonlinear influence on hillslope behavior. As a reminder, the $\cos^2\theta$ factor is a consequence of the lofting and settling process in which the lofting generates a sine dependency and the settling a cosine dependency, so writing (21) and (22) in terms of surface slope leads to the $\cos^2\theta$ factor. To illustrate the effect of this factor we use a one-dimensional vertically integrated statement of conservation [*Mudd and Furbish*, 2004; *Paola and Voller*, 2005; *Heimsath et al.*, 2005] to obtain

$$-D^*\frac{\partial}{\partial x}\left(h\cos^2\theta\frac{\partial\zeta}{\partial x}\right)+\overline{c}\frac{\partial\zeta}{\partial t}=(c_\eta-\overline{c})p_\eta+\overline{c}W, \qquad (45)$$

where W is the uplift rate. In the steady-state case ($\partial\zeta/\partial t = \partial\eta/\partial t = 0$ and $\partial h/\partial x = 0$) where the rate of stream incision at the lower hillslope boundary balances the rate of uplift W, this lower boundary is fixed in a global reference frame, and (45) becomes

$$\frac{\partial}{\partial x}\left(\cos^2\theta\frac{\partial\zeta}{\partial x}\right)=-\frac{c_\eta W}{hD^*}. \qquad (46)$$

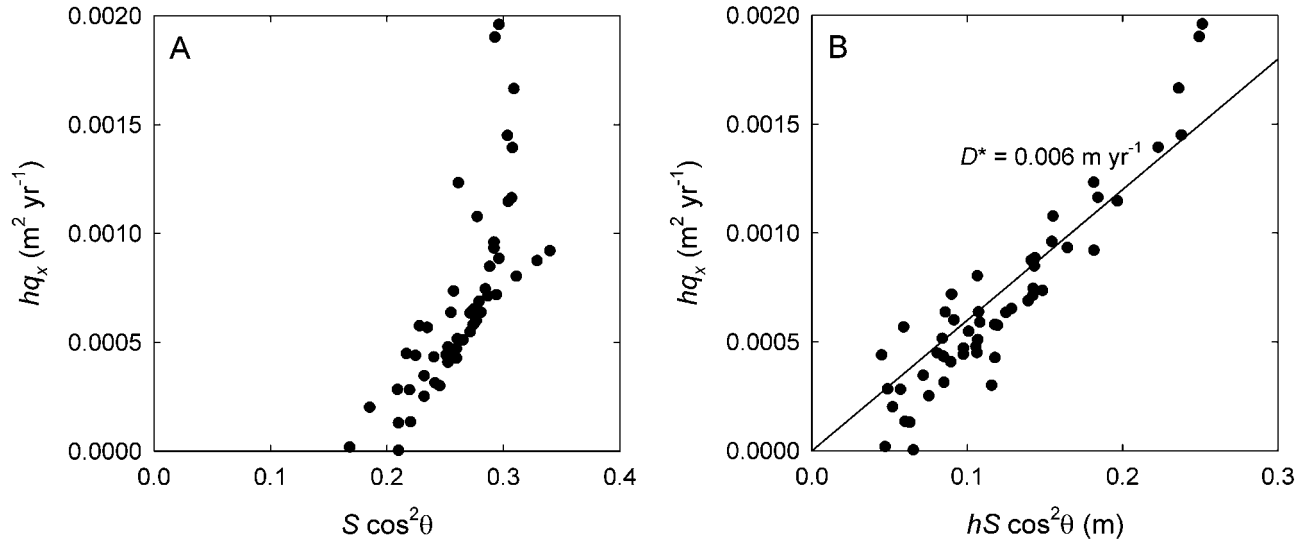

Figure 7. Plot of soil flux $h\overline{q}_x$ (a) versus slope factor $S\cos^2\theta$ and (b) versus the product of soil thickness and slope factor $hS\cos^2\theta$; data for the Nunnock River site taken from *Heimsath et al.* [2005].

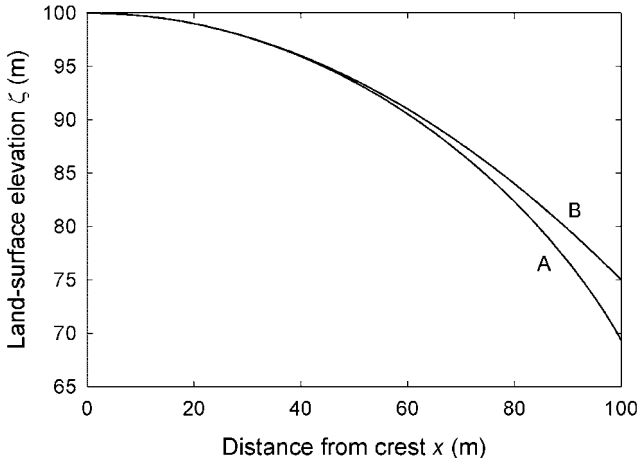

Figure 8. Hillslope profiles at steady state showing land-surface elevation ζ versus distance from crest x with (line a) and without (line b) geometric factor $\cos^2\theta$.

The solution of (46)

$$\zeta(x) = \zeta(0) + \frac{hD^*}{2c_\eta W}\left[(\ln 2 - 1) + \sqrt{1 - 4\left(\frac{c_\eta W}{hD^*}\right)^2 x^2} - \ln\left(1 + \sqrt{1 - 4\left(\frac{c_\eta W}{hD^*}\right)^2 x^2}\right)\right] \quad (47)$$

is nearly parabolic for small x ($\cos^2\theta \sim 1$) but "overly" steepens with distance from the hillslope crest (Figure 8) because of the increasing significance of the factor $\cos^2\theta$.

[46] Using this steady-state case as an initial condition, numerical solutions of (45) with $W = 0$ and a fixed lower boundary suggest that uniform lowering persists over much of the hillslope, as the hillslope does not initially "feel" the influence of the lower boundary, except close to it. Here the soil thickens and the slope decreases. This response then expands upslope with time. Moreover, the rate at which this response propagates upslope is slightly slower than in the case not involving the factor $\cos^2\theta$, and, consistent with the results of *Furbish* [2003] and *Mudd and Furbish* [2007], significantly slower than in the case involving a linear soil transport relation. With soil thickening, soil production decreases and the total soil mass that is exported per unit time at the lower boundary decreases. In the case of linear transport, this is directly matched by decreasing land-surface slope. In the case where transport is proportional to the product of the active soil thickness and land-surface slope, then because soil thickening partially accommodates transport in addition to slope, the rate at which the land surface responds upslope is slowed relative to the rate involving only changes in slope.

5.3. Soil Bulk Density Profiles

[47] The bulk density profiles in Figure 4 (noting that the volumetric concentration $c = \rho_b/\rho_s$) may hold important information regarding the disturbance signals contributing to soil transport at these sites. The profiles from Marin County, California (Figure 4a), and from Washington and Oregon (Figure 4b), are in colluvial fills. Colluvium is transported in and down the hollows associated with dilational disturbances, so the biologically active region is continuously disturbed as accretion occurs, on the order of 1 mm/a due to topographic convergence. Soil material is thus stirred but progressively finds itself farther from the surface where some consolidation may occur. The least noisy signal is from the Marin grassland site, where disturbances are mostly due to gophers. Estimates of soil production from nearby [*Heimsath et al.*, 1997] suggest that production, and thus disturbances, extend to 0.8 m. Thus, near the surface (<0.5 m), bulk density values are highly variable with depth, but are generally smallest near the surface (with smaller values in the wetter, more organic rich, forested soils of Washington and Oregon (Figure 4b)). The bulk density progressively increases with depth to about 1−1.5 m, below which it is more-or-less uniform. These hollow-fill soils thus appear to reveal the full dilational disturbance profile, not just effects of consolidation, and delineate a trend more clearly than could be obtained from, say, a thin soil on the source ridge.

[48] The profiles from Tennessee (Figure 4c) involve thinner soils on three low-relief, convex-concave forested hillslopes. Like the California, Oregon and Washington soils (Figures 4a and 4b), bulk density generally increases with depth, but is highly variable over most of the soil thickness. (Noting the different scales, the variability over the top 0.5 m in Figure 4c is similar to the variability over this same depth in Figures 4a and 4b). Disturbances are mostly due to root growth and the activity of worms, beetles, etc., although the profiles also may reflect remnant effects of tree throw. The profiles from Point Reyes, California (Figure 4d), in contrast, are relatively uniform, with an abrupt change at the soil-saprolite interface (~1 m), suggesting that these soils are continually well stirred. Indeed, estimates of soil production at Point Reyes [*Heimsath et al.*, 2005] indicate that disturbances extend to more than a meter, perhaps reflecting a relatively high overall disturbance frequency. A similar profile of nearly uniform soil bulk density and abrupt increase in bulk density in the saprolite and weathered rock was reported by *Anderson et al.* [2002, Figure 3] for a steep, recently deforested hillslope in the Oregon Coast Range. They also report grain density and porosity, and show through chemical analysis that nearly all of the bulk-density decrease and porosity increase is due to dilational disturbance, as compared to solute loss. In their organic-rich soils, porosity varied from 60% to greater than 80% near the surface.

[49] These profiles of soil bulk density presumably reflect snapshots of a complex process which, when time averaged, involves a balance between the dilational production of porosity (i.e., lofting) by biological activity and the loss of porosity with particle rearrangement via settling and pore collapse. Smooth descriptions of the profiles of particle activity N_a and concentration c, like (35) and (36), therefore must be viewed as representing conditions averaged over many disturbances. Similarly, the smooth displacement profiles in Figure 5 must be viewed as representing time-averaged conditions. Moreover, inasmuch as relatively high-porosity (near-surface) sites in a soil are mechanically "easier" to disturb or are more susceptible to being disturbed than are low-porosity (deeper) sites, then from this point of view the bulk density profiles reflect not only the

availability of pore spaces to accommodate settling motions, but also the distribution of disturbances creating porosity and soil transport. If so, this might open the possibility of using the concentration profile c/c_m to infer a value of the coefficient D^* if a characteristic activity, say $N_{a\zeta}$, is known independently.

6. Discussion and Conclusions

[50] A key idea in the formulation above is that the collective, horizontal (downslope) flux over the active soil thickness consists of the aggregate of the vertical component of the settling motions of particles into open pore space, following slope-normal lofting. That is, gravity does not enter this problem as an effect arising from its downslope component, i.e., $g\sin\theta$, an idea that is more akin to fluid-like behavior. Indeed, locally within the soil, a particle does not even "see" the surface slope above. Rather, the key is that lofting motions normal to the surface slope have a horizontal component, and gravity does the rest. In this formulation any downslope bias in settling motions is a higher-order effect that might arise from upslope-downslope asymmetry in pore structure (and thus net settling distances).

[51] The description of particle motions as consisting of either scattering motions or systematic settling motions provides a useful way to conceptualize the balance of fluxes that occurs in the idealization of steady, uniform soil creep (Figure 3). In the natural setting these motions are intermittent, where locally a soil experiences alternating states of lofting and settling, including production and collapse of macropores, such that at any instant these fluxes are imbalanced. The idea of a balance between particle fluxes that tend to loft a soil and the gravitational settling of particles into available pore space must therefore be viewed as a condition obtained by averaging over many lofting/settling "events." This averaging necessarily involves a time scale spanning many disturbances due to, for example, biological activity or freeze-thaw cycles.

[52] Our use of the probabilistic formalism of the Master equation and the Fokker-Planck equation to describe the volumetric (particle) flux $\mathbf{q}$ provides a concise way to incorporate the idea of intermittent particle activity via the probability $a(\mathbf{x}, t)$, and the idea of different modes of motion via the probability $M_j(\mathbf{x}, t)$. This formulation also highlights that the flux includes both advective and diffusive parts [*Culling*, 1963, 1981] (a result that is particularly important in characterizing the mixing of soil constituents, including distinct particle fractions, or elements and compounds, adsorbed to particles) although our analysis, in aiming at a kinematic description of the flux q_x and the diffusion-like coefficient D, is subsequently simplified in focusing only on the advective part of settling motions. Indeed, in this formulation the settling flux is key. So although the analysis rests on balancing the vertical flux of settling motions with other motions whose net effect is lofting, details of these lofting motions are not critical.

[53] The analysis suggests that for geometrical reasons the vertically integrated soil flux $h\overline{q}_x$ depends on the land-surface slope, multiplied by the factor $\cos^2\theta$. The significance of land-surface slope is that it is a measure of the downslope component of slope-normal lofting that is balanced by settling. In turn the diffusion-like coefficient D includes the active soil thickness h, a characteristic particle size R, the porosity in excess of the consolidated porosity $(1 - c/c_m)$, and the rate of particle activation N_a as a function of depth. These last two ingredients, vertical porosity structure and activation rate, in effect characterize the magnitude and frequency of settling particle motions, and thereby set the rate constant of the transport process.

[54] Because the coefficient D explicitly contains the active soil thickness, the analysis suggests that the soil flux is proportional to the product of this active thickness and slope. This result is consistent with the data provided by *McKean et al.* [1993], but owing to the small variation in soil thickness at the study site, the data cannot distinguish between this possibility and the hypothesis that the flux is simply proportional to land-surface slope. Reproducing the data for the Nannuck River site from *Heimsath et al.* [2005] and incorporating the geometrical factor $\cos^2\theta$, the data in this case are consistent with the hypothesis that the flux is proportional to the product of active soil thickness and slope. Including the factor $\cos^2\theta$, however, does not significantly change the original plot presented by *Heimsath et al.* [2005].

[55] Because D and D^* are vertically integrated quantities, it is not be surprising that D contains the active soil thickness h as one of its characteristic length scales, and that D^* may also vary with h in relation to the vertical structure of particle activation and porosity. The analysis in section 4.2 provides a simple view of how this structure might influence the flux profile $q_x(z)$ (Figure 5), highlighting the importance of the particle activation rate N_a [e.g., *Roering*, 2008]. Nonetheless, the behavior of D^* hinges on how the settling probability M_2 is related via (27) to the particle concentration c. So although the results are consistent with displacement profiles for various creep mechanisms compiled by *Roering* [2004], the analysis remains heuristic given the uncertainty in M_2.

[56] That D and D^* are vertically integrated quantities also suggests that, within the context of a slope-dependent transport relation like (2) or (30), the active soil thickness h provides a minimum length scale over which measurements of surface slope, say $\Delta\zeta/\Delta x$, are meaningful. With $\Delta x \leq h$, the slope measurement is at the same scale as the vertical aggregate of disturbances that produce soil motion, and likely at the same scale as associated surface roughness, whereas the idea of a diffusion-like (slope dependent) model is applicable at scales larger than the disturbances producing the transport [*Jyotsna and Haff*, 1997].

[57] For soil creep over weathered bedrock, entrainment of mass may be partly limited by the weathering rate inasmuch as weathered material must become sufficiently mechanically weak before it can become incorporated within the creeping motion. For soil creep on unconsolidated sediment, the material is mechanically "entrainable" to some depth below the actively creeping soil, and entrainment is thus limited by the mechanisms producing the creep. In the case of bioturbation-driven creep, for example, the active soil thickness therefore may be determined by the depth of biological activity [e.g., *Roering et al.*, 2002b; *Gabet et al.*, 2003; *Roering*, 2008]. With uniform active soil thickness set by this depth, a soil flux that is nominally proportional to the product of thickness and slope would appear to vary only with slope, as in (1).

[58] The active soil thickness h does not necessarily coincide with the soil thickness as defined in a pedological sense [*Yoo and Mudd*, 2008]. For this reason it may be difficult in some situations to determine h precisely, particularly with cumulic soils [e.g., *Birkeland*, 1984] where pedological soil properties, for example, organic carbon content, extend lower in the horizon than they otherwise would in the absence of creep (and accumulation of transported soil material). Field measurements like those of *McKean et al.* [1993] involving vertical profiles of accumulated cosmogenic isotopes, and those of *Heimsath et al.* [2002] involving optically stimulated particles, might be used indirectly to determine the active depth of creep. But we must await a clearer theory of the mechanisms of soil creep to obtain h without such measurements.

[59] The local flux $q_x(z)$ as described by (29) involves the assumption that scattering motions do not have a slope-parallel advective part. Whereas this is reasonable for motions created by small animals and root growth "deep" within the soil, soil material moved close to and on the surface may well involve a downslope bias, which is certainly the case for soil excavated by rodents [*Gabet*, 2000; *Yoo et al.*, 2005]. Following the development above (section 3), a horizontal advective flux due to scattering motions would appear as $q_{x1} = q_{x'1}\cos\theta \sim N_a M_1 u_1' \cos\theta = N_a(c/c_m)u_1'\cos\theta$, where u_1' is the advective speed parallel to the downslope coordinate x' (Figure 3). This flux would be additive to (29). In turn, the speed u_1' may well depend on several quantities, that is, $u_1' = u_1'(c, c_\eta, z, \partial\zeta/\partial x, \ldots)$. The formulation is thus likely most relevant to situations not involving significant downslope surface transport, and possibly gentle slopes (<30°).

[60] The analysis provides insight into probabilistic ingredients of slope-dependent transport, leading to a transport formula that is linear with surface slope. An important open question is how the analysis might mesh with formulations that are consistent with evidence that the flux increases nonlinearly with slope [e.g., *Roering et al.*, 1999, 2002a]. We suspect an answer to this question will emerge from generalized descriptions of particle motions that more completely take into account the full range of motions (magnitude and soil amounts) occurring at pore, macropore and larger scales, perhaps involving the formalism of heavy-tail displacement distributions currently being applied to sediment transport problems (e.g., Bradley et al., submitted manuscript, 2009; Ganti et al., submitted manuscript, 2009; K. M. Hill et al., Particle size dependence of the probability distribution functions of travel distances of gravel particles in bedload transport, submitted to *Journal of Geophysical Research*, 2009).

Appendix A: Specialized Master Equation

[61] The Master equation as written in (9) looks like classic forms of the ME, except that it contains the probability $a(\mathbf{x}, t)$ and modes of motion $M_j(\mathbf{x}, t)$, and classic forms do not. For completeness we therefore present here an abbreviated derivation of the classic ME, then show how a and M_j are incorporated.

[62] As stated in the text, let $f(\mathbf{x}, t)$ denote the probability density associated with the coordinate vector $\mathbf{x}$ of particle position. If with $j = 1$ all particles are in motion, then during $\mathrm{d}t$ the change in the density $f(\mathbf{x}, t)$ may be expressed as [*Ebeling and Sokolov*, 2005]

$$f(\mathbf{x}, t+\mathrm{d}t) - f(\mathbf{x}, t) = \int_{-\infty}^{\infty} f(\mathbf{x}', t) W(\mathbf{x}, t+\mathrm{d}t|\mathbf{x}', t)\mathrm{d}\mathbf{x}' - \int_{-\infty}^{\infty} f(\mathbf{x}, t) W(\mathbf{x}', t+\mathrm{d}t|\mathbf{x}, t)\mathrm{d}\mathbf{x}'. \quad \text{(A1)}$$

This has an intuitively appealing interpretation. Namely, if $W(\mathbf{x}, t + \mathrm{d}t|\mathbf{x}', t)\mathrm{d}\mathbf{x}'$ is a transition probability that a particle is at position $\mathbf{x}$ at time $t + \mathrm{d}t$ given that it was at position $\mathbf{x}'$ at time t, and if $W(\mathbf{x}', t + \mathrm{d}t|\mathbf{x}, t)\mathrm{d}\mathbf{x}'$ is a transition probability that a particle is at position $\mathbf{x}'$ at time $t + \mathrm{d}t$ given that it was at position $\mathbf{x}$ at time t, then the first integral in (A1) represents the movement of particles from all possible positions $\mathbf{x}'$ at time t to the position $\mathbf{x}$ during $\mathrm{d}t$, and the second integral in (A1) represents the movement of particles from the position $\mathbf{x}$ at time t to all possible positions $\mathbf{x}'$ during $\mathrm{d}t$. With respect to position $\mathbf{x}$, therefore, particles arriving at $\mathbf{x}$ during $\mathrm{d}t$ (the first integral) minus particles leaving $\mathbf{x}$ during $\mathrm{d}t$ (the second integral) equals the change in the number of particles at $\mathbf{x}$ during $\mathrm{d}t$ (the left side of (A1)).

[63] As elaborated below, the transition probability W is actually a probability density function, so by definition,

$$\int_{-\infty}^{\infty} W(\mathbf{x}', t+\mathrm{d}t|\mathbf{x}, t)\mathrm{d}\mathbf{x}' = 1. \quad \text{(A2)}$$

Because $f(\mathbf{x}, t)$ in the second integral in (A1) does not depend on $\mathbf{x}'$, this density therefore may be removed from the integral, whence, according to (A2),

$$f(\mathbf{x}, t+\mathrm{d}t) - f(\mathbf{x}, t) = \int_{-\infty}^{\infty} f(\mathbf{x}', t) W(\mathbf{x}, t+\mathrm{d}t|\mathbf{x}', t)\mathrm{d}\mathbf{x}' - f(\mathbf{x}, t). \quad \text{(A3)}$$

Here, W is defined by

$$W(\mathbf{x}, t+\mathrm{d}t|\mathbf{x}', t) = \frac{p(\mathbf{x}', t; \mathbf{x}, t+\mathrm{d}t)}{f(\mathbf{x}', t)}, \quad \text{(A4)}$$

where $p(\mathbf{x}', t; \mathbf{x}, t + \mathrm{d}t)$ is the joint probability density that a particle is at position $\mathbf{x}'$ at time t and at position $\mathbf{x}$ at time $t + \mathrm{d}t$. The conditional density W satisfies the condition that

$$\int_{-\infty}^{\infty} W(\mathbf{x}, t+\mathrm{d}t|\mathbf{x}', t)\mathrm{d}\mathbf{x}' = 1. \quad \text{(A5)}$$

Moreover,

$$W(\mathbf{x}, t|\mathbf{x}', t) = \delta(\mathbf{x} - \mathbf{x}'), \quad \text{(A6)}$$

where δ is the Dirac function.

[64] According to the definition of the Dirac function,

$$\int_{-\infty}^{\infty} \delta(\mathbf{x}' - \mathbf{x})\mathrm{d}\mathbf{x}' = 1, \quad \text{(A7)}$$

so

$$\int_{-\infty}^{\infty} f(\mathbf{x}',t)\delta(\mathbf{x}'-\mathbf{x})\mathrm{d}\mathbf{x}' = f(\mathbf{x},t)\int_{-\infty}^{\infty}\delta(\mathbf{x}'-\mathbf{x})\mathrm{d}\mathbf{x}' = f(\mathbf{x},t), \tag{A8}$$

where placing $f(\mathbf{x}, t)$ outside the integral is justified in that $\delta(\mathbf{x}' - \mathbf{x}) = 0$ for $\mathbf{x} \neq \mathbf{x}'$. Reversing the steps in (A8) we may therefore rewrite (A3) as

$$f(\mathbf{x},t+\mathrm{d}t) - f(\mathbf{x},t) = \int_{-\infty}^{\infty} f(\mathbf{x}',t) \cdot [W(\mathbf{x},t+\mathrm{d}t|\mathbf{x}',t) - \delta(\mathbf{x}'-\mathbf{x})]\mathrm{d}\mathbf{x}'. \tag{A9}$$

Dividing (A9) by $\mathrm{d}t$ and taking the limit as $\mathrm{d}t \to 0$ then leads to the classic ME

$$\frac{\partial f(\mathbf{x},t)}{\partial t} = \int_{-\infty}^{\infty} f(\mathbf{x}',t)V(\mathbf{x},\mathbf{x}',t), \tag{A10}$$

which is like (9), but without the probability $a(\mathbf{x}, t)$ and modes of motion $M_j(\mathbf{x}, t)$.

[65] At any instant only some of the particles at any position $\mathbf{x}$ are in motion, and the others are at rest. Let $a(\mathbf{x}, t)$ denote the proportion of particles at $f(\mathbf{x}, t)$ that are in motion during the small interval $\mathrm{d}t$. As such, $a(\mathbf{x}, t)$ is a pure probability (carrying no physical units). The probability that particles are at rest is $1 - a(\mathbf{x}, t)$. If the joint probability density $p(\mathbf{x}', t; \mathbf{x}, t + \mathrm{d}t)$ in (A4) pertains to both particles in motion and at rest, then

$$\int_{-\infty}^{\infty} p(\mathbf{x}',t;\mathbf{x},t+\mathrm{d}t)\mathrm{d}\mathbf{x} = f(\mathbf{x}',t) \tag{A11}$$

and

$$\int_{-\infty}^{\infty} p(\mathbf{x}',t;\mathbf{x},t+\mathrm{d}t)\mathrm{d}\mathbf{x}' = f(\mathbf{x},t+\mathrm{d}t), \tag{A12}$$

which are the marginal distributions of p. If instead the density $p(\mathbf{x}', t; \mathbf{x}, t + \mathrm{d}t)$ pertains only to particles in motion specifically involving mode M_j, then

$$\int_{-\infty}^{\infty} p(\mathbf{x}',t;\mathbf{x},t+\mathrm{d}t)\mathrm{d}\mathbf{x} = f(\mathbf{x}',t)a(\mathbf{x}',t)M_j(\mathbf{x}',t) \tag{A13}$$

and

$$\int_{-\infty}^{\infty} p(\mathbf{x}',t;\mathbf{x},t+\mathrm{d}t)\mathrm{d}\mathbf{x}' = (f(\mathbf{x},t+\mathrm{d}t) - f(\mathbf{x},t)[1-a(\mathbf{x},t)]) \cdot M_j(\mathbf{x},t). \tag{A14}$$

The right side of (A13) may be interpreted as the proportion of the density $f(\mathbf{x}', t)$ of particles at position $\mathbf{x}'$ that are active at time t involving mode M_j and move to all possible positions $\mathbf{x}$ during $\mathrm{d}t$. The parenthetical part of the right side of (A14) may be interpreted as the proportion of the density $f(\mathbf{x}, t + \mathrm{d}t)$ of all particles residing at position $\mathbf{x}$ at time $t + \mathrm{d}t$, minus those grains that were at $\mathbf{x}$ at time t and remained there during $\mathrm{d}t$. This difference thus represents particle motions to position $\mathbf{x}$ from all possible positions $\mathbf{x}'$ during $\mathrm{d}t$ involving mode M_j.

[66] We now redefine the conditional probability density W in (A4) as

$$W_j(\mathbf{x},t+\mathrm{d}t|\mathbf{x}',t) = \frac{p(\mathbf{x}',t;\mathbf{x},t+\mathrm{d}t)}{f(\mathbf{x}',t)a(\mathbf{x}',t)M_j(\mathbf{x}',t)}, \tag{A15}$$

which pertains only to active grains. That is, whereas p in (A4) is conditioned by all grains at position $\mathbf{x}'$ at time t, all of which, represented by $f(\mathbf{x}', t)$, are assumed to be in motion in the classic formulation, p in (A15) is conditioned by the proportion of active grains at position $\mathbf{x}'$ at time t involving mode M_j, represented by $f(\mathbf{x}', t)a(\mathbf{x}', t)M_j(\mathbf{x}', t)$, understanding that some grains remain at rest. If by chance, with $j = 1$, all grains are active, $a = 1$ and (A15) becomes (A4).

[67] According to (A14), multiplying both sides of (A15) by $f(\mathbf{x}', t)a(\mathbf{x}', t)M_j(\mathbf{x}', t)$ and integrating leads to

$$[f(\mathbf{x},t+\mathrm{d}t) - f(\mathbf{x},t)]M_j(\mathbf{x},t) = \int_{-\infty}^{\infty} f(\mathbf{x}',t)a(\mathbf{x}',t)M_j(\mathbf{x}',t) \times W_j(\mathbf{x},t+\mathrm{d}t|\mathbf{x}',t)\mathrm{d}\mathbf{x}' - f(\mathbf{x},t)a(\mathbf{x},t)M_j(\mathbf{x},t). \tag{A16}$$

Summing over j modes,

$$f(\mathbf{x},t+\mathrm{d}t) - f(\mathbf{x},t) = \int_{-\infty}^{\infty} f(\mathbf{x}',t)a(\mathbf{x}',t)\sum\nolimits_j M_j(\mathbf{x}',t) \times W_j(\mathbf{x},t+\mathrm{d}t|\mathbf{x}',t)\mathrm{d}\mathbf{x}' - f(\mathbf{x},t)a(\mathbf{x},t), \tag{A17}$$

which is analogous to (A3). Moreover, the conditional density W still satisfies (A5) and (A6), so we may rewrite (A17) as

$$f(\mathbf{x},t+\mathrm{d}t) - f(\mathbf{x},t) = \int_{-\infty}^{\infty} f(\mathbf{x}',t)a(\mathbf{x}',t)\sum\nolimits_j M_j(\mathbf{x}',t) \times \left[W_j(\mathbf{x},t+\mathrm{d}t|\mathbf{x}',t) - \delta(\mathbf{x}'-\mathbf{x})\right]\mathrm{d}\mathbf{x}'. \tag{A18}$$

Dividing (A18) by $\mathrm{d}t$ and taking the limit as $\mathrm{d}t \to 0$ then leads to (9) in the text, namely

$$\frac{\partial f(\mathbf{x},t)}{\partial t} = \int_{-\infty}^{\infty} f(\mathbf{x}',t)a(\mathbf{x}',t)\sum\nolimits_j M_j(\mathbf{x}',t)V_j(\mathbf{x},\mathbf{x}',t),$$

where $V(\mathbf{x}, \mathbf{x}', t)$ is defined by (10). The form of $V_j(\mathbf{x}, \mathbf{x}', t)$ must be obtained from dynamical arguments or empirically, and therefore depends on the particular system and mode j. In the present context, (9) explicitly takes into account different possible modes of particle motion, and the fact that, unlike molecular behavior in fluid systems, particles in soils alternate between states of motion and rest.

Appendix B: Specialized Fokker-Planck Equation

[68] The differential form of the ME [*Chandrasekhar*, 1943; *Risken*, 1984], namely (11) in the text, is obtained as follows. The probability that a particle is at position $\mathbf{x}$ at

time $t + \mathrm{d}t$ given that it was at position $\mathbf{x}'$ at time t is identical to the probability that a particle, starting from position $\mathbf{x} - \mathbf{r}$, moves a distance $\mathbf{r} = \mathbf{x} - \mathbf{x}'$ during $\mathrm{d}t$. The function W_j therefore can be reinterpreted as a local probability density of particle hop distances $\mathbf{r}$. Note that $W_j(\mathbf{x}, t + \mathrm{d}t|\mathbf{x}', t) = W_j(\mathbf{x}' + \mathbf{r}, t + \mathrm{d}t|\mathbf{x}', t)$, and we denote this as $U_j(\mathbf{x}', \mathbf{r}; t, \mathrm{d}t)$ [*Eberling and Sokolov*, 2005]. With this we may rewrite (A17) as

$$f(\mathbf{x}, t + \mathrm{d}t) - f(\mathbf{x}, t) = \int_{-\infty}^{\infty} f(\mathbf{x} - \mathbf{r}, t) a(\mathbf{x} - \mathbf{r}, t) \times \sum_j M_j(\mathbf{x} - \mathbf{r}, t) U_j(\mathbf{x} - \mathbf{r}, \mathbf{r}; t, \mathrm{d}t) \mathrm{d}\mathbf{r} - f(\mathbf{x}, t) a(\mathbf{x}, t), \quad \text{(B1)}$$

where geometrically $\mathrm{d}\mathbf{x}' = \mathrm{d}\mathbf{r}$. If U_j is a peaked function near $\mathbf{r} = 0$, and if U_j and f vary smoothly over $\mathbf{x}$, then the integrand in (B1) can be expanded as a Taylor series with respect to $\mathbf{r}$ to give

$$f(\mathbf{x} - \mathbf{r}, t) a(\mathbf{x} - \mathbf{r}, t) \sum_j M_j(\mathbf{x} - \mathbf{r}, t) U_j(\mathbf{x} - \mathbf{r}, \mathbf{r}; t, \mathrm{d}t) \mathrm{d}\mathbf{r} = \left(1 - \mathbf{r}\frac{\partial}{\partial \mathbf{x}} + \frac{\mathbf{r}^2}{2}\frac{\partial^2}{\partial \mathbf{x}^2} - \ldots\right) f(\mathbf{x}, t) a(\mathbf{x}, t) \cdot \sum_j M_j(\mathbf{x}, t) U_j(\mathbf{x}, \mathbf{r}; t, \mathrm{d}t). \quad \text{(B2)}$$

Substitution of the right side of (B2) into (B1) then gives

$$\begin{aligned} f(\mathbf{x}, t + \mathrm{d}t) - f(\mathbf{x}, t) &= -f(\mathbf{x}, t) a(\mathbf{x}, t) + f(\mathbf{x}, t) a(\mathbf{x}, t) \\ &\sum_j M_j(\mathbf{x}, t) \int_{-\infty}^{\infty} U_j(\mathbf{x}, \mathbf{r}; t, \mathrm{d}t) \mathrm{d}\mathbf{r} \\ &- \frac{\partial}{\partial \mathbf{x}} \left[f(\mathbf{x}, t) a(\mathbf{x}, t) \sum_j M_j(\mathbf{x}, t) \int_{-\infty}^{\infty} \mathbf{r} U_j(\mathbf{x}, \mathbf{r}; t, \mathrm{d}t) \mathrm{d}\mathbf{r} \right] \\ &+ \frac{1}{2}\frac{\partial^2}{\partial \mathbf{x}^2} \left[f(\mathbf{x}, t) a(\mathbf{x}, t) \sum_j M_j(\mathbf{x}, t) \int_{-\infty}^{\infty} \mathbf{r}^2 U_j(\mathbf{x}, \mathbf{r}; t, \mathrm{d}t) \mathrm{d}\mathbf{r} \right] \\ &- \ldots . \end{aligned} \quad \text{(B3)}$$

Like W_j, the transition probability density U_j satisfies (A5), so the first two terms on the right side of (B3) cancel. Dividing (B3) by $\mathrm{d}t$ and taking the limit as $\mathrm{d}t \to 0$ then leads to the differential form of the ME, namely (11)

$$\frac{\partial f(\mathbf{x}, t)}{\partial t} = -\frac{\partial}{\partial \mathbf{x}} \left(fa \sum_j M_j m_{1j} \right) + \frac{1}{2}\frac{\partial^2}{\partial \mathbf{x}^2} \left(fa \sum_j M_j m_{2j} \right) - \ldots,$$

where the moments m_{ij} are

$$m_{ij}(\mathbf{x}, t) = \lim_{\mathrm{d}t \to 0} \frac{1}{\mathrm{d}t} \int_{-\infty}^{\infty} \mathbf{r}^i U_j(\mathbf{x}, \mathbf{r}; t, \mathrm{d}t) \mathrm{d}\mathbf{r}. \quad \text{(B4)}$$

[69] Either the first two terms on the right side of (11) are sufficient for a full description of $f(\mathbf{x}, t)$, or the full infinite series must be used. For diffusion-like processes (including classic Brownian motion), only the first two moments in (11) are non-zero. Truncated at second order (11) is the Fokker-Planck (FP) equation, where m_{1j} and m_{2j} are interpreted, respectively, as the grain drift velocity $\mathbf{u}_j$ and the diffusion (or dispersion) coefficient tensor $\mathbf{D}_j$, so

$$\frac{\partial f(\mathbf{x}, t)}{\partial t} = -\frac{\partial}{\partial \mathbf{x}} \left(fa \sum_j M_j \mathbf{u}_j \right) + \frac{1}{2}\frac{\partial^2}{\partial \mathbf{x}^2} \left(fa \sum_j M_j \mathbf{D}_j \right). \quad \text{(B5)}$$

Note that when this is written as a divergence

$$\frac{\partial f(\mathbf{x}, t)}{\partial t} = -\frac{\partial}{\partial \mathbf{x}} \left[fa \sum_j M_j \mathbf{u}_j - \frac{1}{2}\frac{\partial}{\partial \mathbf{x}} \left(fa \sum_j M_j \mathbf{D}_j \right) \right] \quad \text{(B6)}$$

it is apparent that the probability flux density

$$\mathbf{q} = q_x \mathbf{i} + q_y \mathbf{j} + q_z \mathbf{k} = fa \sum_j M_j \mathbf{u}_j - \frac{1}{2}\frac{\partial}{\partial \mathbf{x}} \left(fa \sum_j M_j \mathbf{D}_j \right), \quad \text{(B7)}$$

where $\mathbf{u}_j$ and $\mathbf{D}_j$ pertain to the motions of active grains (not involving rest times).

[70] Let $n(\mathbf{x}, t)$ denote the number concentration (or number density) of grains measured as a number per unit volume. For a closed system with N grains, $n(\mathbf{x}, t) = Nf(\mathbf{x}, t)$, and for an open system, $n(\mathbf{x}, t) = N(t)f(\mathbf{x}, t)$. Let $n(\mathbf{x}, t) = n[f(\mathbf{x}, t)]$. Then $\mathrm{d}n/\mathrm{d}t = (\mathrm{d}n/\mathrm{d}f)\partial f/\partial t = N\partial f/\partial t$. As N may be a function of time, but not space, multiplying (B5) through by N then leads to

$$\frac{\partial n(\mathbf{x}, t)}{\partial t} = -\frac{\partial}{\partial \mathbf{x}} \left(na \sum_j M_j \mathbf{u}_j \right) + \frac{1}{2}\frac{\partial^2}{\partial \mathbf{x}^2} \left(na \sum_j M_j \mathbf{D}_j \right). \quad \text{(B8)}$$

This can be readily converted to involve other measures of concentration (e.g., volume or mass of grains per unit volume) by multiplying through by an appropriate factor (e.g., the volume or mass per grain).

Appendix C: Magnitude of Advective Versus Dispersive Settling

[71] With reference to (23) it is useful to introduce the following dimensionless quantities denoted by circumflexes

$$z = h\hat{z}, \quad a = a_\zeta \hat{a}, \quad M_2 = M_{2\zeta}\hat{M}_2, \quad c = C\hat{c}, \quad w_2 = w_{2\zeta}\hat{w}_2 \quad \text{and} \quad D_2 = D_{2\zeta}\hat{D}_2, \quad \text{(C1)}$$

where a_ζ and $M_{2\zeta}$ denote values of the activity probability a and the settling probability M_2 at the soil surface, $C = c_\eta - c_\zeta$, and $w_{2\zeta}$ and $D_{2\zeta}$ denote values of w_2 and D_2 at the soil surface. Substituting the expressions in (C1) into (23) leads to

$$q_{z2} = w_{2\zeta} a_\zeta M_{2\zeta} C \hat{w}_2 \hat{a} \hat{M}_2 \hat{c} - \frac{D_{2\zeta} a_\zeta M_{2\zeta} C}{2h} \frac{\partial}{\partial \hat{z}} \left(\hat{D}_2 \hat{a} \hat{M}_2 \hat{c} \right). \quad \text{(C2)}$$

Comparing the leading coefficients on the advective and diffusive terms, it is apparent that the latter term, using (24), can be neglected when

$$\frac{D_{2\zeta}}{w_{2\zeta}h} \sim \frac{k_2 l_\zeta}{h} \ll 1. \tag{C3}$$

The dimensionless ratio $w_{2\zeta}h/D_{2\zeta} \sim h/k_2 l_\zeta$ is a Peclet number, and suggests that the advective term dominates when the average settling motion near the soil surface is significantly less than the active soil depth.

Notation

a particle activity probability.
$\hat{a}$ dimensionless particle activity probability.
a_ζ particle activity probability at soil surface.
A elementary plane segment [L^2].
b cube edge [L].
c volumetric particle concentration, $c = 1 - \varphi = \rho_b/\rho_s$.
c_B concentration of ^{10}Be [M^{-1}].
$c_{B\eta}$ concentration of ^{10}Be at base of active soil [M^{-1}].
c_m natural consolidated (maximum) volumetric particle concentration.
c_M mass concentration [M L^{-3}].
$\hat{c}$ dimensionless volumetric particle concentration.
c_η volumetric particle concentration at base of active soil.
c_ζ volumetric particle concentration at soil surface.
$\overline{c}$ vertically averaged volumetric particle concentration.
C characteristic volumetric particle concentration, $C = c_\eta - c_\zeta$.
D diffusion-like coefficient [L^2 t^{-1}].
D_j local diffusion-like coefficient for jth mode of motion [L^2 t^{-1}].
$\hat{D}_2$ dimensionless diffusion-like coefficient associated with particle settling.
$D_{2\zeta}$ diffusion-like coefficient associated with particle settling at soil surface [L^2 t^{-1}].
D^* quasi-local transport coefficient [L t^{-1}].
$\mathbf{D}_j$ diffusion-like coefficient tensor [L^2 t^{-1}].
$f(\mathbf{x}, t)$ probability density of particle position [L^{-3}].
h local thickness of active soil, $h = \zeta - \eta$ [L]; hydraulic head [L].
H characteristic soil thickness [L].
H_1 Heaviside step function.
$\mathbf{i}, \mathbf{j}, \mathbf{k}$ unit vectors parallel to Cartesian coordinates x, y, and z.
k, k_2 dimensionless coefficients.
K_c kinematic mass diffusivity [L^2 t^{-1}].
K_h hydraulic conductivity [L t^{-1}].
K_T thermal conductivity [M L T^{-1} t^{-3}].
l mean free path [L].
L particle translation distance [L].
m_{1j}, m_{2j} first and second probability moments of jth mode of motion [L t^{-1}] and [L^2 t^{-1}].
M_j probability of jth mode of motion.
$\hat{M}_2$ dimensionless probability of settling motion.
$M_{2\zeta}$ probability of settling motion at soil surface.
n number concentration (or number density) [L^{-3}].
N number of particles; number of particle interactions.
N_a particle activation rate [t^{-1}].
N_V number of particles per unit volume [L^{-3}].
N_{Vm} number of particles per unit volume at consolidated density [L^{-3}].
N_m number of particle interactions at consolidated density.
p_η rate of soil production, or rate of entrainment or disentrainment at base of active soil [L t^{-1}].
P nominal rate of soil production when $h \rightarrow 0$ [L t^{-1}].
P_B ^{10}Be deposition rate per unit area [L^{-2}].
$\mathbf{q}$ local volumetric flux density, $\mathbf{q} = \mathbf{i}q_x + \mathbf{j}q_y + \mathbf{k}q_z$ [L t^{-1}].
$\mathbf{q}_c$ mass flux density [M L^{-2} t^{-1}].
$\mathbf{q}_h$ water volume flux density (or specific discharge) [L t^{-1}].
$\mathbf{q}_s$ volumetric flux per unit contour distance, $\mathbf{q}_s = (h/c_\eta)\overline{\mathbf{q}}$ [L^2 t^{-1}].
$\mathbf{q}_T$ heat flux density [M t^{-3}].
q_x, q_y, q_z local volumetric flux density components parallel to x, y and z [L t^{-1}].
$\overline{\mathbf{q}}$ vertically averaged volumetric flux density, $\overline{\mathbf{q}} = \mathbf{i}\overline{q}_x + \mathbf{j}\overline{q}_y$ [L t^{-1}].
$\overline{q}_x, \overline{q}_y$ vertically averaged volumetric flux density components parallel to x and y [L t^{-1}].
$\mathbf{r}$ particle displacement distance [L].
R characteristic particle radius [L].
t time [t].
T temperature [T].
T_R average soil particle residence time scale, $T_R = H/p_\eta$ [t].
T_X diffusive time scale of hillslope with length X, $T_X = X^2/D$ [t].
u particle speed parallel to x [L t^{-1}].
u'_1 advective particle speed parallel to inclined coordinate x' [L t^{-1}].
$\mathbf{u}_j$ particle drift velocity [L t^{-1}].
$\overline{u}_a$ average speed of active particles [L t^{-1}].
$\overline{u}_A$ average virtual speed of particles [L t^{-1}].
U probability density of displacement distance $\mathbf{r}$ [L^{-1}].
V transition rate probability.
w particle speed parallel to z [L t^{-1}].
$\hat{w}_2$ dimensionless settling speed [L t^{-1}].
$w_{2\zeta}$ settling speed at soil surface [L t^{-1}].
W tectonic uplift rate [L t^{-1}].
W_j conditional probability density of jth mode of motion.
x, y, z Cartesian coordinates [L].
$\mathbf{x}, \mathbf{x}'$ coordinate vector, $\mathbf{x} = (x, y, z)$, $\mathbf{x}' = (x', y', z')$ [L].
X hillslope length, downslope distance [L].
$\hat{z}$ dimensionless vertical coordinate.
α characteristic length scale of particle activation rate [L].
β characteristic length scale of particle concentration [L].

γ characteristic length scale in soil production function [L].
$\delta(\mathbf{x} - \mathbf{x}')$ Dirac function.
ζ local coordinate position of land surface [L].
η local coordinate position of base of active soil [L].
θ angle of land-surface slope.
κ vertical component of particle displacement distance $\mathbf{r}$ [L].
$\overline{\kappa}$ average settling displacement [L].
ρ_b soil bulk density [M L^{-3}].
ρ_p, ρ_s particle density [M L^{-3}].
τ small time interval [t].
ϕ soil porosity.
ψ depth beneath surface, $\psi = \zeta - z$ [L].
∇ three-dimensional gradient operator, $\nabla = \mathbf{i}\partial/\partial x + \mathbf{j}\partial/\partial y + \mathbf{k}\partial/\partial z$ [L^{-1}].
∇_2 two-dimensional gradient operator, $\nabla_2 = \mathbf{i}\partial/\partial x + \mathbf{j}\partial/\partial y$ [L^{-1}].

[72] **Acknowledgments.** We appreciate thoughtful discussions with Lesley Glass, Simon Mudd, Chris Paola, Mark Schmeeckle, and Nikki Strong. Three anonymous reviewers provided valuable input. This work was supported in part by the National Science Foundation (EAR-0405119 and EAR-0744934). We dedicate this paper to William E. H. Culling in honor and memory of his pioneering work on soil creep.

References

Abrahams, A. D., A. J. Parsons, and J. Wainwright (1995), Effects of vegetation change on interrill runoff and erosion, Walnut Gulch, southern Arizona, *Geomorphology*, *13*, 37–48.

Ahnert, F. (1967), The role of the equilibrium concept in the interpretation of landforms of fluvial erosion and deposition, in *L'Evolution des Versants*, edited by P. Macar, pp. 23–41, Univ. of Liege, Liege, Belgium.

Anderson, R. S. (2002), Modeling of tor-dotted crests, bedrock edges and parabolic profiles of the high alpine surfaces of the Wind River Range, Wyoming, *Geomorphology*, *46*, 35–58.

Anderson, S. P., W. E. Dietrich, and G. H. Brimhall Jr. (2002), Weathering profiles, mass-balance analysis, and rates of solute loss: Linkages between weathering and erosion in a small, steep catchment, *Geol. Soc. Am. Bull.*, *114*, 1143–1158.

Benson, D. A., S. W. Wheatcraft, and M. M. Meerschaert (2000a), The fractional-order governing equation of Lévy motion, *Water Resour. Res.*, *36*, 1413–1423.

Benson, D. A., S. W. Wheatcraft, and M. M. Meerschaert (2000b), Application of a fractional advection-dispersion equation, *Water Resour. Res.*, *36*, 1403–1412.

Benson, D. A., R. Schumer, S. W. Wheatcraft, and M. M. Meerschaert (2001), Fractional dispersion, Lévy motion, and the MADE tracer tests, *Transp. Porous Media*, *42*, 211–240.

Birkeland, P. W. (1984), *Soils and Geomorphology*, Oxford Univ. Press, Oxford, U. K.

Bochet, E., J. Poesen, and J. L. Rubio (2000), Mound development as an interaction of individual plants with soil, water erosion and sedimentation processes on slopes, *Earth Surf. Processes Landforms*, *25*, 847–867.

Bucknam, R. C., and R. E. Anderson (1979), Estimation of fault-scarp ages from a scarp-height-slope-angle relationship, *Geology*, *7*, 11–14.

Carson, M. A., and M. J. Kirkby (1972), *Hillslope Form and Process*, Cambridge Univ. Press, Cambridge, U. K.

Chandrasekhar, S. (1943), Stochastic problems in physics and astronomy, *Rev. Mod. Phys.*, *15*, 1–89.

Childs, E. M. (2008), Rainsplash as an advection-dispersion process, with implications for plant-soil interactions in arid environments, M.S. thesis, Vanderbilt Univ., Nashville, Tenn.

Clarke, M. F., M. A. J. Williams, and T. Stokes (1999), Soil creep: Problems raised by a 23 year study in Australia, *Earth Surf. Processes Landforms*, *24*, 151–175.

Covey, A. K. (2008), Effects of earthworm burrowing on arsenic biotransformation and mobility: Implications for roxarsone-bearing poultry litter application, M.S. thesis, Vanderbilt Univ., Nashville, Tenn.

Culling, W. E. H. (1960), Analytical theory of erosion, *J. Geol.*, *68*, 336–344.

Culling, W. E. H. (1963), Soil creep and the development of hillside slopes, *J. Geol.*, *71*, 127–161.

Culling, W. E. H. (1965), Theory of erosion on soil-covered slopes, *J. Geol.*, *73*, 230–254.

Culling, W. E. H. (1981), New methods of measurement of slow particulate transport processes on hillside slopes, in *Proceedings of the Florence Symposium, Erosion and Sediment Transport Measurement, 22–26 June 1981*, *Int. Assoc. Hydrol. Sci. Publ.*, vol. 133, pp. , 267–274, Int. Assoc. of Hydrol. Sci. Press, Wallingford, U. K.

Darcy, H. (1856), *Les Fontaines Publiques de la Ville de Dijon*, Dalmont, Paris.

Davison, C. (1889), On the creeping of the soil-cap through the action of frost, *Geol. Mag.*, *6*, 255–261.

Dietrich, W. E., R. Reiss, M. Hsu, and D. R. Montgomery (1995), A process-based model for colluvial soil depth and shallow landsliding using digital elevation data, *Hydrol. Processes*, *9*, 383–400.

Dietrich, W. E., D. Bellugi, A. M. Heimsath, J. J. Roering, L. Sklar, and J. D. Stock (2003), Geomorphic transport laws for predicting landscape form and dynamics, in *Prediction in Geomorphology*, *Geophys. Monogr. Ser.*, vol. 135, edited by P. Wilcock and R. Iverson, pp. 103–132, doi:10.1029/135GM09, AGU, Washington, D. C.

Ebeling, W., and I. M. Sokolov (2005), *Statistical Thermodynamics and Stochastic Theory of Nonequilibrium Systems*, *Ser. Adv. Stat. Mech.*, vol. 8, World Sci., Hackensack, N. J.

Fernandes, N. F., and W. E. Dietrich (1997), Hillslope evolution by diffusive processes: The timescale for equilibrium adjustments, *Water Resour. Res.*, *33*, 1307–1318.

Fick, A. (1855), Über diffusion, Ann. Phys, *Chem.*, *94*, 59–86.

Fourier, J. (1822), *Théorie Analytique de la Chaleur*, Didot, Paris.

Furbish, D. J. (2003), Using the dynamically coupled behavior of land-surface geometry and soil thickness in developing and testing hillslope evolution models, in *Prediction in Geomorphology*, *Geophys. Monogr. Ser.*, vol. 135, edited by P. Wilcock and R. Iverson, pp. 169–181, AGU, Washington, D. C.

Furbish, D. J., and S. Fagherazzi (2001), Stability of creeping soil and implications for hillslope evolution, *Water Resour. Res.*, *37*, 2607–2618.

Furbish, D. J., M. W. Schmeeckle, and J. J. Roering (2008), Thermal and force-chain effects in an experimental, sloping granular shear flow, *Earth Surf. Processes Landforms*, *33*, 2108–2177, doi:10.1002/esp.1655.

Gabet, E. J. (2000), Gopher bioturbation: Field evidence for nonlinear hillslope diffusion, *Earth Surf. Processes Landforms*, *25*, 1419–1428.

Gabet, E. J., O. J. Reichman, and E. W. Seabloom (2003), The effects of bioturbation on soil processes and sediment transport, *Ann. Rev. Earth Planet. Sci.*, *31*, 249–273.

Hanks, T. C., R. C. Bucknam, K. R. Lajoie, and R. E. Wallace (1984), Modification of wave-cut and faulting-controlled landforms, *J. Geophys. Res.*, *89*, 5771–5790.

Heimsath, A. M., W. E. Dietrich, K. Nishiizumi, and R. C. Finkel (1997), The soil production function and landscape equilibrium, *Nature*, *388*, 358–361.

Heimsath, A. M., W. E. Dietrich, K. Nishiizumi, and R. C. Finkel (1999), Cosmogenic nuclides, topography, and the spatial variation of soil depth, *Geomorphology*, *27*, 151–172.

Heimsath, A. M., J. C. Chappell, N. A. Spooner, and D. G. Questiaux (2002), Creeping soil, *Geology*, *30*, 111–114.

Heimsath, A. M., D. J. Furbish, and W. E. Dietrich (2005), The illusion of diffusion: Field evidence for depth-dependent sediment transport, *Geology*, *33*, 949–952.

Hirano, M. (1975), Simulation of developmental process of interfluvial slopes with reference to graded form, *J. Geol.*, *83*, 113–123.

Jeans, J. (1960), *An Introduction to the Kinetic Theory of Gases*, Cambridge Univ. Press, Cambridge, U. K.

Jyotsna, R., and P. K. Haff (1997), Microtopography as an indicator of modern hillslope diffusivity in arid terrain, *Geology*, *25*, 695–698.

Kaste, J. M., A. M. Heimsath, and B. C. Bostick (2007), Short-term soil mixing quantified with fallout radionuclides, *Geology*, *35*, 243–246, doi:10.1130/G23355A.1.

Kirkby, M. J. (1967), Measurement and theory of soil creep, *J. Geol.*, *75*, 359–378.

Kojan, E. (1967), Mechanics and rates of natural soil creep, paper presented at 5th Annual Engineering Geology and Soils Engineering Symposium, Idaho Dep. of Highways, Pocotello, Idaho.

Martin, Y., and M. Church (1997), Diffusion in landscape development models: On the nature of basic transport relations, *Earth Surf. Processes Landforms*, *22*, 273–279.

McKean, J. A., W. E. Dietrich, R. C. Finkel, J. R. Southon, and M. W. Caffee (1993), Quantification of soil production and downslope creep rates from cosmogenic ^{10}Be accumulations on a hillslope profile, *Geology*, *21*, 343–346.

Mitchell, J. K., R. G. Campanella, and A. Singh (1968), Soil creep as a rate process, *J. Soil Mech. Found. Div. Am. Soc. Civ. Eng.*, *94*, 231–253.

Mudd, S. M., and D. J. Furbish (2004), Influence of chemical denudation on hillslope morphology, *J. Geophys. Res.*, *109*, F02001, doi:10.1029/2003JF000087.

Mudd, S. M., and D. J. Furbish (2007), Responses of soil mantled hillslopes to transient channel incision rates, *J. Geophys. Res.*, *112*, F03S18, doi:10.1029/2006JF000516.

Nash, D. (1980a), Forms of bluffs degraded for different lengths of time in Emmet County, Michigan, U.S.A., *Earth Surf. Processes Landforms*, *5*, 331–345.

Nash, D. (1980b), Morphological dating of degraded normal fault scarps, *J. Geol.*, *88*, 353–360.

Nikora, V., H. Habersack, T. Huber, and I. McEwan (2002), On bed particle diffusion in gravel bed flows under weak bed load transport, *Water Resour. Res.*, *38*(6), 1081, doi:10.1029/2001WR000513.

Paola, C., and V. R. Voller (2005), A generalized Exner equation for sediment mass balance, *J. Geophys. Res.*, *110*, F04014, doi:10.1029/2004JF000274.

Parsons, A. J., A. D. Abrahams, and J. R. Simanton (1992), Microtopography and soil-surface materials on semi-arid piedmont hillslopes, southern Arizona, *J. Arid Environ.*, *22*, 107–115.

Reneau, S. L. (1988), Depositional and erosional history of hollows: Application to landslide location and frequency, long term erosion rates and the effects of climate change, Ph.D. dissertation, Univ. of Calif., Berkeley, Calif.

Reneau, S. L., and W. E. Dietrich (1987), Size and location of colluvial landslides in a steep forested landscape, in *Proceedings of the International Symposium on Erosion and Sedimentation in the Pacific Rim, 3–7 August 1987, Corvallis, Oregon*, *Int. Assoc. Hydrol. Sci. Publ.*, vol. 165, pp., 39–48, Int. Assoc. of Hydrol. Sci. Press, Wallingford, U. K.

Reneau, S. L., and W. E. Dietrich (1991), Erosion rates in the southern Oregon Coast Range: evidence for an equilibrium between hillslope erosion and sediment yield, *Earth Surf. Processes Landforms*, *16*, 307–322.

Reneau, S. L., W. E. Dietrich, C. J. Wilson, and J. D. Rogers (1984), Colluvial deposits and associated landslides in the northern Bay Area, S.F., California, USA, in *Proceedings of the IVth International Symposium on Landslides, Toronto, 1984*, pp. 425–430, Univ. of Toronto Press, Toronto, Ont., Canada.

Reneau, S. L., W. E. Dietrich, M. Rubin, D. J. Donahue, and J. T. Jull (1989), Analysis of hillslope erosion rates using dated colluvial deposits, *J. Geol.*, *97*, 45–63.

Risken, H. (1984), *The Fokker-Planck Equation: Methods of Solution and Applications*, Springer, Berlin.

Roering, J. J. (2004), Soil creep and convex-upward velocity profiles: Theoretical and experimental investigation of disturbance-driven sediment transport on hillslopes, *Earth Surf. Processes Landforms*, *29*, 1597–1612.

Roering, J. J. (2008), How well can hillslope models "explain" topography? Simulating soil transport and production with high-resolution topographic data, *Geol. Soc. Am. Bull.*, *120*, 1248–1262, doi:10.1130/B26283.1.

Roering, J. J., J. W. Kirchner, and W. E. Dietrich (1999), Evidence for nonlinear, diffusive sediment transport on hillslopes and implications for landscape morphology, *Water Resour. Res.*, *35*, 853–870.

Roering, J. J., J. W. Kirchner, and W. E. Dietrich (2001), Hillslope evolution by nonlinear slope-dependent transport: Steady-state morphology and equilibrium adjustment timescales, *J. Geophys. Res.*, *106*, 16,499–16,513.

Roering, J. J., J. W. Kirchner, L. S. Sklar, and W. E. Dietrich (2002a), REPLY: Hillslope evolution by nonlinear creep and landsliding: An experimental study, *Geology*, *30*, 482.

Roering, J. J., P. Almond, P. Tonkin, and J. McKean (2002b), Soil transport driven by biological processes over millennial time scales, *Geology*, *30*, 1115–1118.

Roering, J. J., P. Almond, P. Tonkin, and J. McKean (2004), Constraining climatic controls on hillslope dynamics using a coupled model for the transport of soil and tracers: Application to loess-mantled hillslopes, Charwell River, South Island, New Zealand, *J. Geophys. Res.*, *109*, F01010, doi:10.1029/2003JF000034.

Roseberry, J. C. (2009), Effects of soil transport processes on organic carbon storage in forested hillslope soils, M.S. thesis, Vanderbilt Univ., Nashville, Tenn.

Roseberry, J. C., and D. J. Furbish (2008), Downslope transport of soil organic carbon on forested hillslopes, *EOS Trans. AGU*, *89*(53), Fall Meet. Suppl., Abstract H51D-0846.

Schumer, R., M. Meerschaert, and B. Baeumer (2009), Fractional advection-dispersion equations for modeling transport at the Earth's surface, *J. Geophys. Res.*, doi:10.1029/2008JF001246, in press.

Schumm, S. A. (1967), Rates of surficial rock creep on hillslopes in western Colorado, *Science*, *155*, 560–562.

Strong, N., and D. J. Furbish (1999), A mechanism for particle size sorting in soil and marine sediments, *Geol. Soc. Am. Abstr. Programs*, *31*, Abstract A53.

Yoo, K., and S. M. Mudd (2008), Toward process-based modeling of geochemical soil formation across diverse landforms: A new mathematical framework, *Geoderma*, *146*, 248–260, doi:10.1016/j.geodema.2008.05.029.

Yoo, K., R. Amundson, A. M. Heimsath, and W. E. Dietrich (2005), Process-based model linking pocket gopher (*Thomomys bottae*) activity to sediment transport and soil thickness, *Geology*, *33*, 917–920, doi:10.1130/G21831.1.

Yoo, K., R. Amundson, A. M. Heimsath, W. E. Dietrich, and G. H. Brimhall (2007), Integration of geochemical mass balance with sediment transport to calculate rates of soil chemical weathering and transport on hillslopes, *J. Geophys. Res.*, *112*, F02013, doi:10.1029/2005JF000402.

W. E. Dietrich, Department of Earth and Planetary Science, University of California, Berkeley, Berkeley, CA 94720, USA. (bill@eps.berkeley.edu)

D. J. Furbish, Department of Earth and Environmental Sciences and Department of Civil and Environmental Engineering, Vanderbilt University, Nashville, TN 37235, USA. (david.j.furbish@vanderbilt.edu)

P. K. Haff, Division of Earth and Ocean Sciences, Nicholas School of the Environment, Duke University, Durham, NC 27708, USA. (haff@duke.edu)

A. M. Heimsath, School of Earth and Space Exploration, Arizona State University, Tempe, AZ 85287, USA. (arjun.heimsath@asu.edu)